České vysoké učení technické v Praze
Fakulta elektrotechnická

Czech Technical University in Prague
Faculty of Electrical Engineering

Doc. Ing. Ivan Zemánek, CSc.

Vybrané problémy měření parametrů otevřených vzorků magneticky měkkých materiálů při střídavém magnetování

Selected Problems of the Open Specimen Measurements of Soft Magnetic Materials Parameters at AC Magnetization

SUMMARY

Soft magnetic materials (classic silicon electrical steel sheets and modern amorphous materials) are ones of the most important construction elements used in the electrical engineering. Their parameters significantly influence the quality of construted equipments. It is a reason for material as exact as possible parameters measurement both during the material check-in or check-out, and during their production.

Magnetic materials are usually produced in forms of “infinite length” strips from which the specimens (small strips or sheets) for stationary measurements are obtained. The strips, sheets and “infinite length” strips represent (magnetic measurements viewpoint) open specimens.

The open strip specimens are usually measured in the Epstein frame. With respect to fundamental, unremovable deficiency of the Epstein frame testing and to elaborateness of strip specimens preparation the development of the open specimen measuring methods in the world unambiguously tends to the single sheet testing (SST) or to on-line testing (OLT) the base of which is magnetizing yoke.

The stationary sheet measurements or on-line measurement of moving strips during the production process, respectively, brings new problems. This lecture deals with some of them and shows the possible solutions.

The problem of the magnetic field strength measurement in the measured material is discussed at first. The original Czech MMF compensation method (developed at the FEE CTU by prof. Mikulec) is presented as a possible solution. The considerations about the magnetic field homogeneity and MMF method accuracy are presented.

The generation of the required magnetic flux density waveform in the measured material (one of defined magnetizing condition) and its keeping at high intensities of magnetizing is the next discussed problem. The design of the special digital correction feedback net is the problem solution.

The demand on the automated measurement of the magnetic materials characteristics and measuring process acceleration at simultaneous keeping of the process convergence reliability in stromg non-linear environment is the third of discussed problems. The regula falsi method and “discrete” Newton´s method, respectively, are found as convenient numerical methods. The logarithm function, Kneppo´s function and exponential function are shown as process accelerating non-linear transformations.

The lecture is completed by actual results of measurements on the systems developed at the Circuit Theory Departmentof the FEE CTU in Prague. These systems became the base for the construction of special measuring equpments for the soft magnetic material testing both in laboratories and in the industrial practice in Rolling Works Frýdek-Místek.

SOUHRN

Magneticky měkké materiály (klasické křemíkové elektrotechnické plechy i moderní amorfní materiály) patří mezi nejdůležitější konstrukční prvky používané v elektrotechnice. Jejich parametry výrazným způsobem ovlivňují kvalitu konstruovaných zařízení. Proto je nutné parametry těchto materiálů co nejpřesněji měřit, jak při vstupní a výstupní kontrole, tak v průběhu jejich výroby.

Magnetické materiály se nejčastěji vyrábějí ve formě "nekonečných" pasů, ze kterých se pro potřeby stacionárních měření získávají vzorky ve formě pásků, či tabulí. Páskové, resp. tabulové vzorky, i samotné pasy představují z hlediska magnetických měření otevřené vzorky.

Měření otevřených vzorků ve formě pásků se obvykle provádí v Epsteinově rámu. S ohledem na principiální a neodstranitelné nedostatky tohoto způsobu měření i vzhledem k pracnosti přípravy páskových vzorků směřuje celosvětový vývoj měření otevřených vzorků ke stacionárním tabulovým, resp. průběžným měřičům, jejichž základem je magnetovací jho.

Stacionární měření tabulí, resp. průběžné měření pohybujících se pasů v procesu výroby, přináší nové problémy. Tato přednáška se zabývá některými z těchto problémů a zároveň ukazuje možnosti řešení.

Nejprve je diskutována problematika měření intenzity magnetického pole v měřeném materiálu. Jako možné řešení je prezentována originální česká kompenzační metoda (vyvinutá na FEL ČVUT prof. Mikulcem). V souvislosti s ní jsou prezentovány úvahy o homogenitě magnetického pole i přesnosti samotné metody.

Přednáška se dále zabývá problémem generování požadovaného časového průběhu magnetické indukce v měřeném materiálu (jedné z definovaných podmínek magnetování) a jeho udržení při vysokých intenzitách magnetování. Řešením problému je návrh speciální digitální korekční zpětnovazební sítě.

Třetím diskutovaným problémem je požadavek automatizovaného měření charakteristik magnetických materiálů a zrychlení měřicího procesu v silně nelineárním prostředí, při současném zajištění spolehlivosti konvergence procesu. Jako vhodná numerická metoda je posuzována metoda regula falsi, resp. diskrétní Newtonova metoda. Jako process urychlující nelineární transformace jsou ukázána logaritmická funkce, Kneppova funkce a exponenciální funkce.

Přenáška je doplněna skutečnými výsledky měření na systémech vyvinuých na katedře teorie obvodů FEL ČVUT. Tyto systémy se staly základem pro konstrukci speciálních měřicích zařízení pro testování magneticky měkkých materiálů jak v laboratorních podmínkách, tak průmyslové praxi ve Válcovnách plechu ve Frýdku-Místku.

Klíčová slova

Magneticky měkké materiály, střídavá magnetická měření, otevřené vzorky, měření intenzity magnetického pole, kompenzační metoda, homogenita magnetického pole, stabilita, přesnost měření, časový průběh magnetické indukce, korekční proces, automatizovaná měření, numerické methody, nelineární transformace, kompenzační ferometry.

Keywords

Soft magnetic materials, AC magnetic measurements, open specimens, magnetic field strength measurement, MMF compensation method, magnetic field homogeneity, stability, measurement accuracy, magnetic flux density waveform, correction process, automated measurements, numerical methods, non-linear transformations, compensation ferrometers.

©, ISBN

CONTENTS

1. INTRODUCTION 6

2. MEASUREMENT OF SOFT MAGNETIC MATERIALS AT AC MAGNETIZATION 7

2.1 Parameters of soft magnetic materials 7

2.2 Measurement of closed specimens 10

2.3 Measurement of open specimens 13

2.3.1 Epstein frame 13

2.3.2 Single sheet testing 15

3. PROBLEMS OF OPEN SPECIMEN MEASUREMENTS 16

3.1 Magnetic field strength measurement 16

3.1.1 IEC method 17

3.1.2 H-coil method 18

3.1.3 MMF compensation method 19

Magnetic field homogeneity 24

MMF compensation metod accuracy 26

3.2 Magnetic flux density waveform 31

3.2.1 Analogue correction 35

3.2.2 Digital correction 36

3.3 Automated measurements 41

4. COMPENSATION FERROMETERS 48

5. CONCLUSION 50

ACKNOWLEDGEMENTS 50

REFERENCES 51

CURRICULUM VITAE 54

1. INTRODUCTION

Magnetic materials are ones of the most important construction materials used in the electrical engineering. The significant of them are soft magnetic materials used in electrical equipments containing magnetic circuits with time varying magnetic flux. The most significant are classic silicon electrical steels and new modern amorphous materials.

Since magnetic properties of used soft magnetic materials have usually a significant influence on parameters of the constructed electrical equipments, it is necessary to evaluate magnetic materials properties by the measurement of important magnetic materials parameters, both during the material check-in or check-out and during the technological process of the material production.

The evaluation of soft magnetic materials properties is a relatively difficult process. For correct and exact soft magnetic materials parameters measurement and for required repeatability of the measurement it is necessary to provide

- exactly defined magnetizing conditions in the measured region of the magnetic material specimen:
  - homogeneous magnetic field
  - required magnetic flux (density) waveform
- correct conversion of magnetic quantities to electrical ones
- exact measurement of electrical quantities (voltage, current, power) at extreme conditions:
  - strong harmonic distortion of magnetizing current
  - low value of power factor

Due to the "whirl" character of the magnetic field expressed by the equation (1.0.1):

$$\operatorname{div} \mathbf{H} = 0\,, \tag{1.0.1}$$

the correct magnetic measurement (without special measuring arrangement) can be carried out on closed material specimens (toroids) only. However magnetic properties of man–made toroidal specimens have low correlation with properties of soft magnetic materials produced usually in the form of strips or sheets. The specially arranged measurement of open specimens (strips, sheets) is therefore very actual theme. Selected problems of the open specimen magnetic measurements at AC magnetization are discussed and their solutions presented in this publication.

2. MEASUREMENT OF SOFT MAGNETIC MATERIALS AT AC MAGNETIZATION

Properties of soft magnetic materials are evaluated by the measurement of important magnetic material parameters at exactly defined magnetizing conditions.

2.1 Parameters of soft magnetic materials

Dynamic hysteresis loop – dependence of the instantaneous value of the magnetic flux density $B(t)$ on the instantaneous value of the magnetic field strength $H(t)$ – is a fundamental soft magnetic materials characteristic:

$$B = \mathrm{f}(H) . \tag{2.1.1}$$

It is measured at standardized AC magnetizing conditions given usually by exactly defined waveform of magnetic flux $\Phi(t)$.

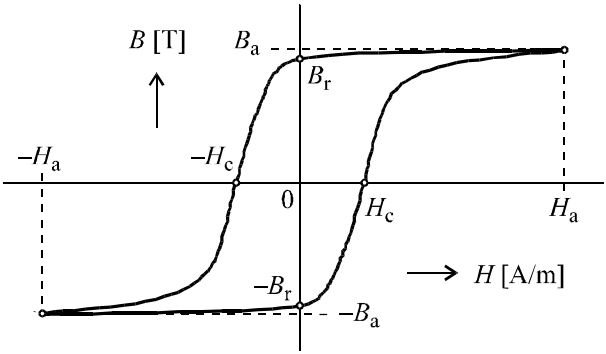

Fig. 2.1.1 Dynamic hysteresis loop

With respect to typical use of soft magnetic materials in practice (silicon electrical steel in most cases) the sinusoidal waveform of magnetic flux $\Phi(t)$ is required in measured material, i.e. sinusoidal waveform of the average magnetic flux density $B(t)$ in the specimen cross-section S with exactly determined amplitude B_a and magnetizing frequency ω:

$$B(t) = \frac{F(t)}{S} = B_a \sin(w t) . \tag{2.1.2}$$

The most important parameter of soft magnetic materials at defined AC magnetizing conditions is a quantity of *specific power losses* [W/kg]. Two basic soft magnetic material characteristics are therefore monitored:

- *amplitude magnetizing characteristic* – dependence of the magnetic flux density amplitude B_a on magnetic field strength amplitude H_a

$$B_a = f_1(H_a) \tag{2.1.3}$$

- dependence of *specific power losses* p on the magnetic flux density amplitude B_a

$$p = f_2(B_a). \tag{2.1.4}$$

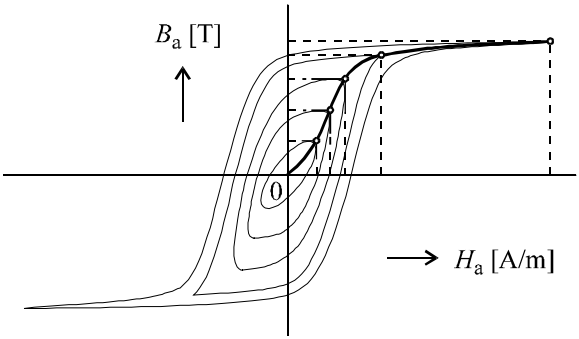

Fig. 2.1.2 Amplitude magnetizing characteristic

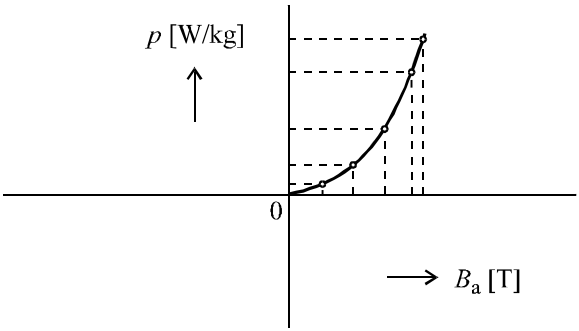

Fig. 2.1.3 Specific power losses

These characteristics are measured in several operating points (H_a) and (B_a), respectively, defined by the soft magnetic material standard. As an example, the standardized operating points for classic silicon oriented electric steels are in Tab. 2.1.1

Tab. 2.1.1 Standardized operating points for oriented electric steel sheets

$B_a = f_1(H_a)$	
H_a [A/m]	B_a [T]
30	…
800	…
1000	…
10000	…

$p = f_2(B_a)$	
B_a [T]	p [W/kg]
1.0	…
1.5	…
1.7	…

In addition to the *hysteresis loop* $B = f(H)$, *amplitude magnetization characteristic* $B_a = f_1(H_a)$ and *specific power losses* $p = f_2(B_a)$, the other important parameters of soft magnetic materials are also usually measured:

- magnetization amplitude J_a [T]
- magnetic remanence B_r [T]
- coercivity H_c [A/m]
- magnetic field strength RMS value H_{RMS} [A/m]
- relative amplitude permeability μ_{ra} [–]
- specific apparent losses s [VA/kg]
- power factor p/s [–]

With respect to the standardized magnetic field strength amplitudes H_a and magnetic flux density ones B_a (some of which presents magnetization up to deep material saturation) the measurement of soft magnetic materials parameters (especially on-line measurement at industrial conditions) is very difficult. Due to strong magnetic materials non-linearity the parameters of magnetic materials (as permeability) change their values in several orders range for different intensities of the magnetization. The achievement and maintenance of the standardized magnetic flux density waveform $B(t)$ at the standardized saturation amplitudes H_a and B_a is practically impossible. In addition the industrial magnetic measurements can be done in an indirect way only by the conversion of magnetic quantities to electrical ones.

2.2 Measurement of closed specimens

The principle of the soft magnetic material parameters measurement at AC magnetization is relatively simple if the measured magnetic material forms toroid (closed magnetic circuit) with small thickness:

$$\frac{r_1}{r_2} \rightarrow 1, \tag{2.2.1}$$

inside of which a homogeneous magnetic field can be supposed (Fig. 2.2.1).

The measured toroidal specimen is magnetized by the magnetizing system GEN – MA – MW (exciting signal generator GEN, magnetizing amplifier MA, magnetizing winding MW).

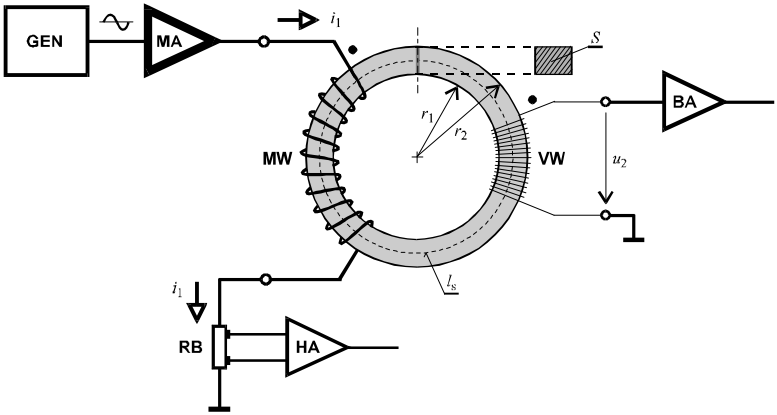

Fig. 2.2.1 Principle of closed specimen measurement

The magnetizing current i_1 (carried by the magnetizing winding MW with N_1 turns) generates approximately homogeneous magnetic field H in the toroidal specimen. Better homogeneity of the magnetic field H can be achieved if the magnetizing winding MW is uniformly distributed along the whole toroidal specimen.

The magnetizing current i_1 is measured by the current shunt RB and measuring amplifier HA. The voltage u_2 induced in the measuring voltage winding VW with N_2 turns is measured by the measuring amplifier BA.

The relations between directly measured electrical quantities i_1 and u_2 and corresponding magnetic ones (magnetic field strength H, magnetic flux density B) are expressed by the basic equations of the electromagnetic field.

According to the 1st Maxwell´s equation:

$$\oint_l \mathbf{H}\,\mathbf{dl} \;=\; N_1\, i_1 \tag{2.2.2}$$

with respect to supposed homogeneity of the magnetic field in the toroidal specimen, the average *magnetic field strength H* can be calculated from the magnetizing current i_1 and mean length of the flux line $l_s = \pi\,(r_1 + r_2)$:

$$H\, l_s \;=\; N_1\, i_1 \tag{2.2.3}$$

$$H(t) \;=\; \frac{N_1\, i_1(t)}{l_s}\,. \tag{2.2.4}$$

The average *magnetic flux density B* in the specimen cross-section *S* can be calculated from the voltage u_2 induced in the voltage winding VW according to the Faraday´s induction law:

$$u_2 \;=\; N_2 \frac{\mathrm{d}F}{\mathrm{d}t} \;=\; N_2 S \frac{\mathrm{d}B}{\mathrm{d}t} \tag{2.2.5}$$

$$B(t) \;=\; \frac{1}{N_2 S} \int_{-\infty}^{t} u_2(\tau)\,\mathrm{d}\tau\,, \tag{2.2.6}$$

and magnetic flux density amplitude B_a from the mean value U_{2s} of the induced voltage u_2 within a half-period:

$$B_{min} \;=\; B(t_1) \qquad\qquad B_{max} \;=\; B(t_2) \tag{2.2.7}$$

$$B_a \;=\; \frac{B_{max} - B_{min}}{2} \;=\; \frac{1}{2N_2 S} \int_{t_1}^{t_2} u_2(\tau)\,\mathrm{d}\tau \;=$$

$$\;=\; \frac{1}{4 f N_2 S} \cdot \frac{2}{T} \int_{t_1}^{t_2} u_2(\tau)\,\mathrm{d}\tau \;=\; \frac{U_{2s}}{4 f N_2 S}\,. \tag{2.2.8}$$

The specific power losses *p* of the magnetic material (at given magnetic flux density amplitude B_a) can be determined from the dynamic hysteresis loop *area* because it represents energy that is necessary for the

remagnetization of the unit volume of the measured magnetic material within one period of the AC magnetization.

$$p = \frac{P}{m} = \frac{P}{rV} = \frac{f}{r} \oint H \, \mathrm{d}B \tag{2.2.9}$$

(P – total power loss in measured material, m – material mass, ρ – material density, V – material volume, f – magnetizing frequency).

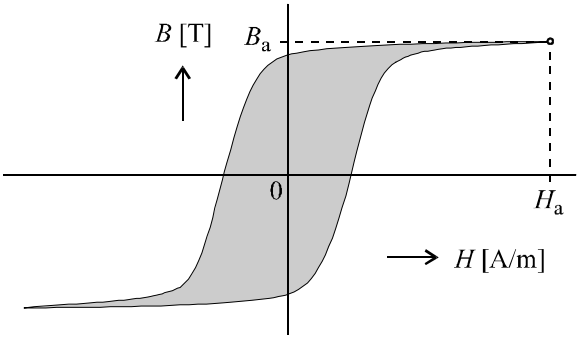

Fig. 2.2.2 Area of the dynamic hysteresis loop

With respect to magnetic field homogeneity in the closed toroidal specimen the magnetic field strength H and magnetic flux density B can be expressed by the eqns (2.2.4) and (2.2.5), respectively. The specific power losses p can be calculated from the active power P_m of the magnetizing current i_1 and induced voltage u_2 :

$$p = \frac{f}{r} \int_0^T \frac{N_1 i_1}{l_\mathrm{s}} \frac{u_2}{N_2 S} \, \mathrm{d}t = \frac{1}{r V} \frac{N_1}{N_2} \frac{1}{T} \int_0^T i_1 \, u_2 \, \mathrm{d}t \tag{2.2.10}$$

$$p = \frac{N_1}{N_2} \frac{P_m}{m} . \tag{2.2.11}$$

However the measurement of the active power P_m at extreme conditions (strong harmonic distortion of the magnetizing current i_1 and low power factor) is relatively difficult.

2.3 Measurement of open specimens

Due to the "whirl" character of the magnetic field (1.0.1) the correct and effective magnetic measurement of open specimens (sheets, strips) without special measuring arrangement is impossible.

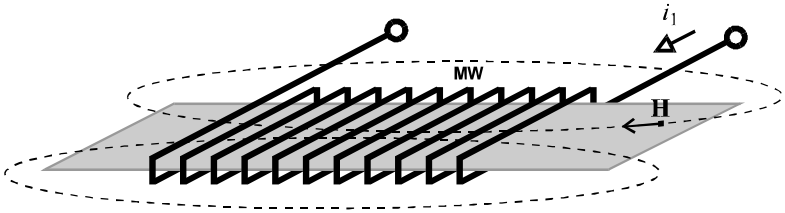

Fig. 2.3.1 Open specimen and magnetic field "whirl" character

The correct measurement of open specimens can be carried out on the artificially man–made closed magnetic circuits only that may be realized by two standardized ways (either / or) [1]:

- arrangement of the set of measured strips to closed magnetic circuit in the Epstein frame (Fig. 2.3.2)
- completing of the measured single sheet or strip by the magnetizing yoke with low reluctance (Fig. 2.3.4) – single sheet testing.

2.3.1 Epstein frame

The Epstein frame is the oldest equipment for the evaluation of magnetic properties of electrical steel strips. Its small version (called small Epstein frame) is used till present. The set of measured strips 30 x 280 mm (total mass of which is 0.5 – 1 kg) is composed in the square frame the closed magnetic circuit with square core to be formed (Fig. 2.3.2). The magnetizing winding MW and voltage one VW are uniformly distributed along the whole man-made closed magnetic circuit.

The strip overlap in the frame corners (making indeterminate magnetic flux transit between overlapped strips – magnetic surface phenomena, undefined air gaps) disables the unambiguous determination of the magnetic circuit length (mean flux line length). This length (presenting the length of the equivalent homogeneous magnetic circuit with the cross-section of one frame jib) actually depends on given magnetizing conditions, measured material and strip thickness. It had being originally determined empirically by the comparing measurements. Later, the small Epstein frame mean flux line length was determined and standardized as l_s = 940 mm. This numerical

value warrants good Epstein frame measurement repeatability and results stability for given standardized conditions only. This is fundamental and non-recoverable Epstein frame deficiency.

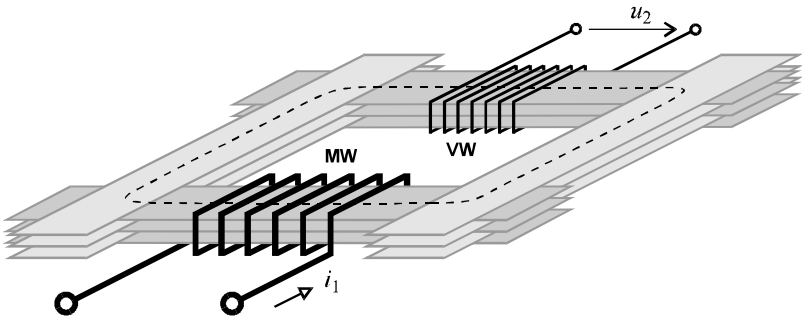

Fig. 2.3.2 Epstein frame

The results of the measurements on the Epstein frame at these conditions are calculated (similary to the closed specimen measurements) from the magnetizing current i_1 and induced voltage u_2.

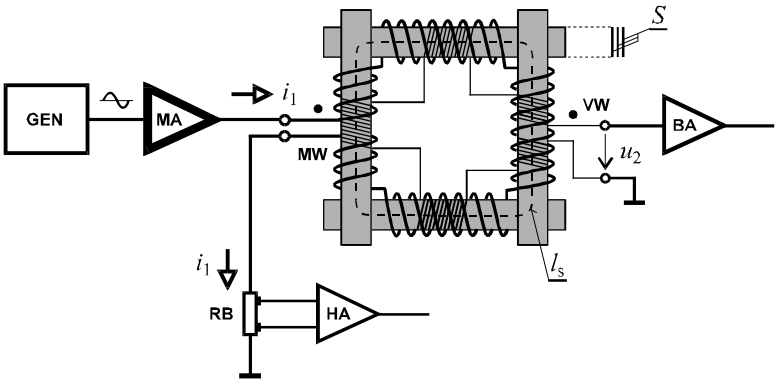

Fig. 2.3.3 Epstein frame measurement

The main Epstain frame advantage is its construction simplicity and acknoledgement as an international AC magnetic measurements standard. With respect to its fundamental deficiency and to other disadvantages – elaborateness of measured strips preparation (cutting, annealing, stacking in the frame), complexity of the measuring procedure – the development of the open specimen measuring methods in the world unambiguously tends to the single sheet testing (SST) or to on principle similar on-line testing (OLT) .

2.3.2 Single sheet testing

The principle of the single sheet testing is in Fig. 2.3.4. The specimen of the measured material S (single sheet) is completed by the magnetizing yoke Y, the closed magnetic circuit (specimen S – air gap G1 – yoke Y – air gap G2) to be formed. Analogous to the toroid testing, the specimen S is wound by the magnetizing winding MW (N_1 turns of thick wire) and by the voltage winding VW (N_2 turns of thin wire closely wound on the specimen).

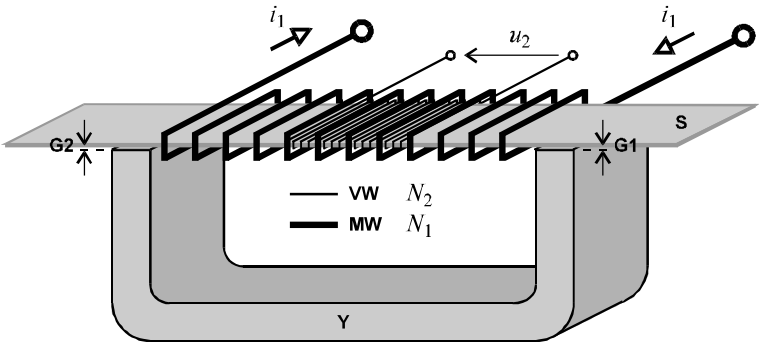

Fig. 2.3.4 Single sheet testing – principle

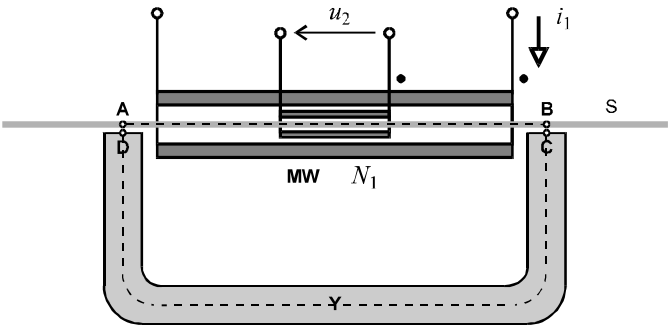

Fig. 2.3.5 Single sheet testing – schematic

The principle of the single sheet testing is similar to the closed-specimen (toroidal) testing or to the Epstein frame one. The magnetizing and measuring electronics is on principle the same. However, the single sheet testing brings several specific problems. These problems and possibilities of their solving are discussed in next chapters.

3. PROBLEMS OF OPEN SPECIMEN MEASUREMENTS

The open specimen measurements bring several specific problems of:

- **magnetic field strength measurement**
  - IEC method
  - H-coil method
  - MMF compensation method
- **magnetic flux density waveform generation**
- **automated measurement**

3.1 Magnetic field strength measurement

The main problem consists in correct evaluation of the magnetic field strength H in the measured material. The magnetizing current i_1 of the magnetizing winding MW with N_1 turns generates the non-homogeneous magnetic field H along the flux line A–B–C–D–A of the magnetic circuit:

$$\oint \mathbf{H}\mathrm{d}\mathbf{l} = \int_{A}^{B} H\,\mathrm{d}l + \int_{B}^{C} H\,\mathrm{d}l + \int_{C}^{D} H\,\mathrm{d}l + \int_{D}^{A} H\,\mathrm{d}l = N_1 i_1 . \qquad (3.1.1)$$

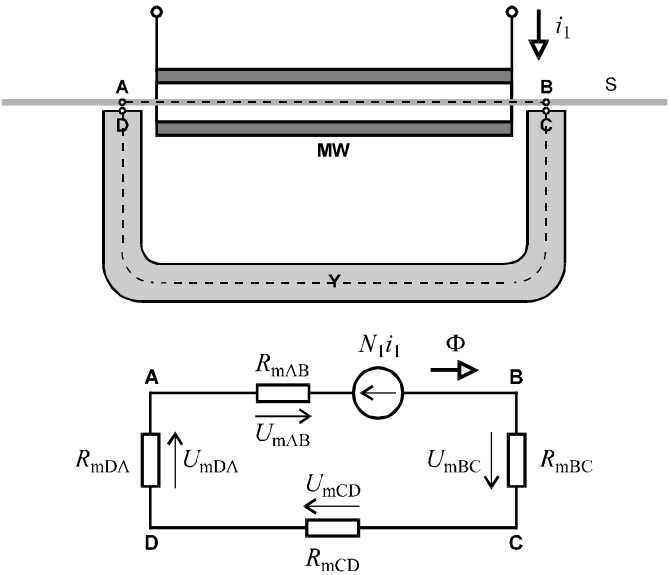

Fig. 3.1.1 Magnetic circuit and its model

Due to the non-homogeneity of the magnetic field in the magnetic circuit the exact distribution of the MMF of the magnetizing winding $N_1 i_1$ along the flux line A–B–C–D–A is not defined. It is impossible to determine the MMF drops across the yoke (U_{mCD}) and uncertain air gaps (U_{mBC} , U_{mDA}) and determine what portion U_{mAB} of the magnetomotive force MMF $N_1 i_m$ „falls" on the measured material.

There are two standardized methods in the world generally used for the open specimen testing magnetic field strength H evaluation:

- IEC method (Europe, USA – for SST)
- H-coil method (Japan – for SST, OLT).

The third one, till now internationally non-standardized method, is

- original Czech MMF compensation method (for SST, OLT).

3.1.1 IEC method

The IEC method uses a special high quality magnetizing yoke with negligible reluctance ($R_{mCD} \approx 0$) and with precise glazed surface of yoke poles to find negligible air gaps B–C and D–A between yoke poles and measured specimen ($R_{mBC} \approx 0$, $R_{mDA} \approx 0$). The MMF drops U_{mCD}, U_{mBC} and U_{mDA} are negligible in this case.

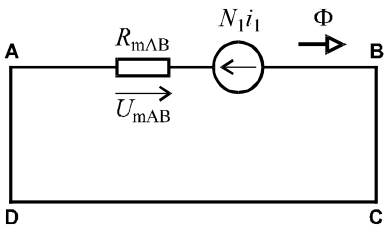

Fig. 3.1.2 Model of the magnetic circuit (IEC method)

The average magnetic field strength in measured region of the specimen can be calculated directly from the magnetizing current i_1 (analogous to the closed (toroid) specimen testing or Epstein testing):

$$\int_A^B H \, \mathrm{d}l = N_1 i_1 \tag{3.1.2}$$

$$\overline{H} \, l_{AB} = N_1 i_1 \quad \Rightarrow \quad \overline{H} = \frac{N_1 i_1}{l_{AB}}. \tag{3.1.3}$$

The disadvantages of the IEC method are:

- extreme requirements on yoke quality
- impossibility of use for on-line testing (OLT).

3.1.2 H-coil method

The H-coil method uses for the H measurement special flat air coil (H-coil) placed just "above" the measured material surface and oriented in the magnetizing direction. The voltage induced in the H-coil is processed and the average magnetic field strength calculated.

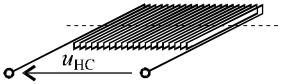

Fig. 3.1.3 H-coil

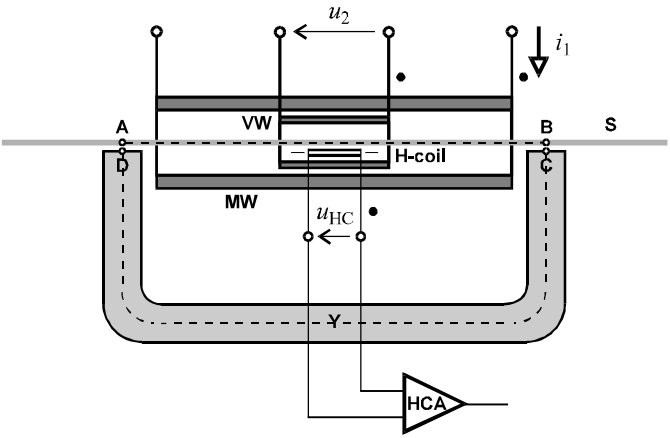

Fig. 3.1.4 H-coil method

$$u_{HC} = K_{HC}\frac{dH}{dt} \quad \Rightarrow \quad H(t) = \frac{1}{K_{HC}}\int_{-\infty}^{t} u_{HC}(\tau)\,d\tau \qquad (3.1.4)$$

The H-coil method disadvantages are:

- robust magnetizing equipment (H-coil(s) must be placed under the voltage winding VW)
- necessity of special signal processing electronics
- necessity of H-coils calibration.

3.1.3 MMF compensation method

The cited disadvatanges of the IEC and H-coil method are overcome by the original Czech MMF compensation method developed at the Czech Technical University in Prague by prof. Mikulec [9], [10]. The principle of the MMF compensation method is shown in Fig. 3.1.5.

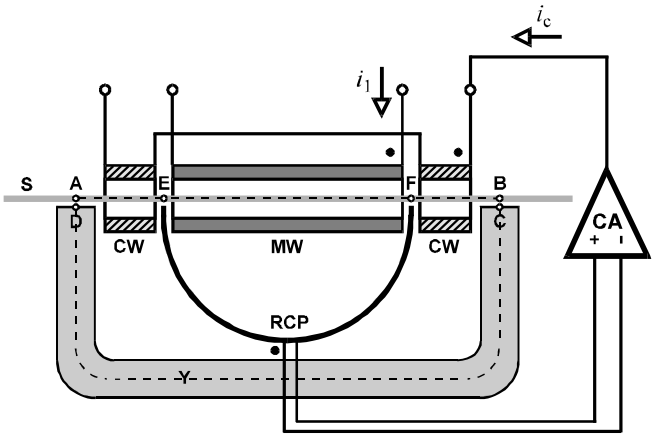

Fig. 3.1.5 Principle of the MMF compensation method

The standard magnetizing equipment (MW, Y) is completed by an extra compensation winding CW-CW with N_c turns (flown by the compensation current i_c of the compensation amplifier CA), and the Rogowski-Chattock potentiometer RCP enclosing N_1 turns of the magnetizing winding MW.

$$\int_A^E H\,\mathrm{d}l + \int_E^F H\,\mathrm{d}l + \int_F^B H\,\mathrm{d}l + \int_B^C H\,\mathrm{d}l + \int_C^D H\,\mathrm{d}l + \int_D^A H\,\mathrm{d}l = N_1 i_1 + N_c i_c \quad (3.1.5)$$

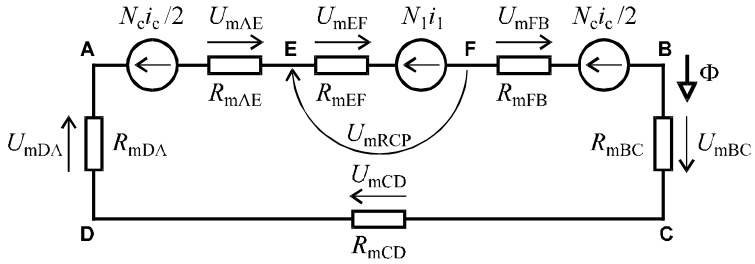

Fig. 3.1.6 Model of the magnetic circuit (MMF compensation method)

The RCP is a special flat coil with high number of turns wound on a non-magnetic „U – formed" core. It measures the MMF drop across the measured region (points E–F) (Fig. 3.1.7).

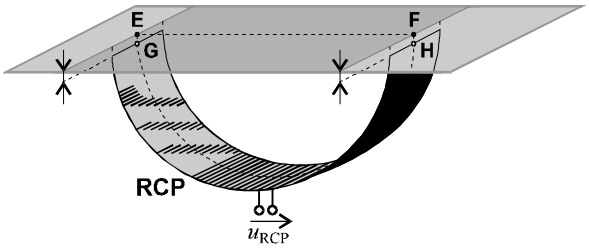

Fig. 3.1.7 RCP measurement of the MMF drop U_{mEF}

$$\oint \mathbf{H}\mathbf{dl} = \underbrace{\int_{F}^{E} H\,dl}_{U_{mEF}} + \underbrace{\int_{E}^{H} H\,dl}_{\approx 0} + \underbrace{\int_{H}^{G} H\,dl}_{U_{mRCP}} + \underbrace{\int_{G}^{F} H\,dl}_{\approx 0} = 0 \qquad (3.1.6)$$

$$U_{mRCP} = -U_{mEF} \qquad (3.1.7)$$

The RCP enclosing N_1 turns of the magnetizing winding measures the difference ΔU_m [10] between the MMF of the magnetizing winding $N_1 i_1$ and actual MMF drop U_{mEF} across the measured region E–F (Fig. 2.1.8).

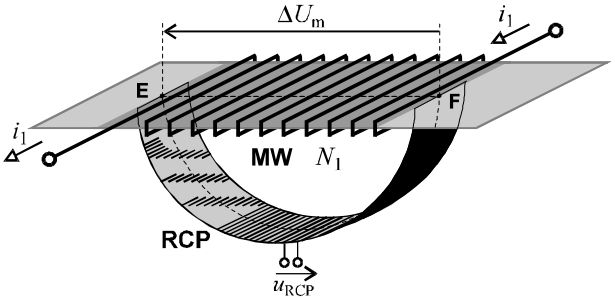

Fig. 3.1.8 RCP measurement of the MMF difference ΔU_m

$$\oint \mathbf{H}\mathbf{dl} = U_{mEF} + U_{mRCP} = N_1 i_1 \qquad (3.1.8)$$

$$U_{mRCP} = N_1 i_1 - U_{mEF} = \Delta U_m \qquad (3.1.9)$$

According to eqns (3.1.5), (3.1.9) the measured MMF diference $\Delta U_m = U_{mRCP}$ represents all MMF drops out of the specimen measured region E–F compensated by the MMF of the compensating winding $N_c i_c$:

$$U_{mRCP} = \int_A^E H\,dl + \int_F^B H\,dl + \int_B^C H\,dl + \int_C^D H\,dl + \int_D^A H\,dl - N_c i_c . \qquad (3.1.10)$$

The RCP is a component of the compensation feedback loop with big amplification factor (RCP – compensation amplifier CA – compensation winding CW-CW). The compensation current i_c is automatically controlled the voltage u_{RCP} induced in the RCP to be zero at any time instant. The RCP serves as a MMF drop zero indicator.

$$u_{RCP} = K_{RCP} \frac{dU_{mRCP}}{dt} \qquad (3.1.11)$$

The derivative character of the RCP (3.1.11) is eliminated by the integration character of the remaining feedback loop components (CA, CW-CW).

In the state of perfect compensation when the MMF drops $\Delta U_m = U_{mRCP}$ are compensated, it is valid:

$$U_{mRCP} = \frac{1}{K_{RCP}} \int u_{RCP}(t)\,dt = 0 \qquad (3.1.12)$$

$$N_1 i_1 - \int_E^F H\,dl = 0 . \qquad (3.1.13)$$

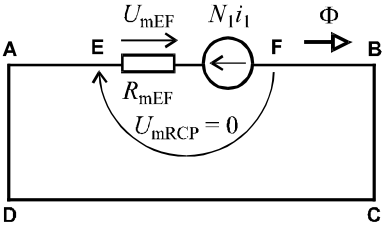

Fig. 3.1.9 Linear model of the magnetic circuit (IEC method)

In this case it is possible to calculate average magnetic field strenth in the measured region E–F from the magnetizing current i_1 and the length of the measured region l_{EF} determined by the RCP poles distance

$$\int_E^F H\,dl = \overline{H}\, l_{EF} = N_1 i_1 \quad \Rightarrow \quad \overline{H} = \frac{N_1 i_1}{l_{EF}} . \qquad (3.1.14)$$

The specific power losses p are:

$$p = \frac{1}{r\, l_{EF} S} \frac{N_1}{N_2} \frac{1}{T} \int_0^T i_1\, u_2\, \mathrm{d}t\,. \qquad (3.1.15)$$

For the actual arrangement of the MMF compensation feedback loop two important facts must be taken into account:

- RCP output signal is electrical voltage u_{RCP} (proportional to differentiation of the measured magnetic voltage (MMF) U_{mRCP}
- CW and MW are connected by common magnetic flux.

With respect to them two basic possible MMF compensation feedback loop structures was designed [10].

In the first structure (Fig. 3.1.10) the voltage u_{RCP} (induced in the RCP) is first of all integrated by the integrator INT. The resulting voltage u_{INT} (proportional to the RCP measured MMF U_{mRCP}) excites the power compensation amplifier CIA and directly controls its output current – compensating current i_c.

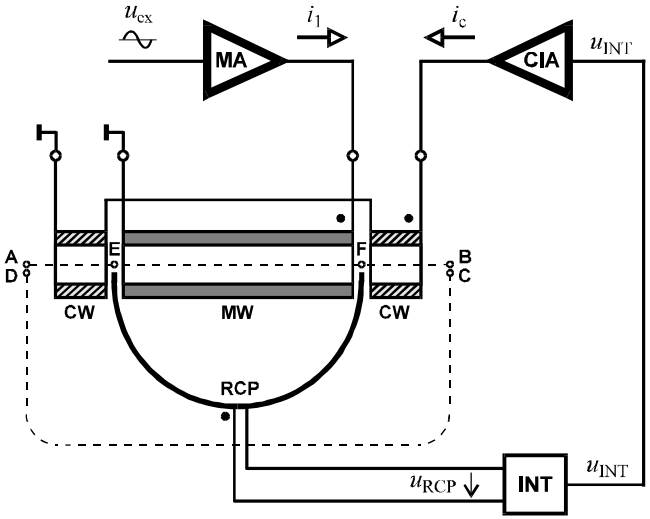

Fig. 3.1.10 MMF compensation loop with CIA

The MMF compensation loop (RCP – INT – CIA – CW-CW) operates as proportional feedback where measured MMF U_{mRCP} is control deviation ($\Delta U_m = U_{mRCP}$). The CIA must operate as a voltage controlled current source loaded by the compensation winding CW-CW. This fact brings unwanted

voltage induction in the compensation winding CW-CW caused by the time variations of the magnetic flux in the magnetizing winding MW. The CIA must be therefore protected against induced voltage impulses caused by transients. Among other things the sensitive integrator INT causes troubles with unwanted additional DC component that must be eliminated.

The second structure (Fig. 3.1.11) overcomes the described troubles. The power compensation amplifier CUA is excited by the combination of the magnetizing voltage u_1 from the magnetizing amplifier MA and preamplified voltage u_{RCP} from the differential preamplifier DA. Both the MA and CUA must operate as a voltage controlled voltage sources. The magnetizing current i_1 and compensation current i_c are dependent quantities.

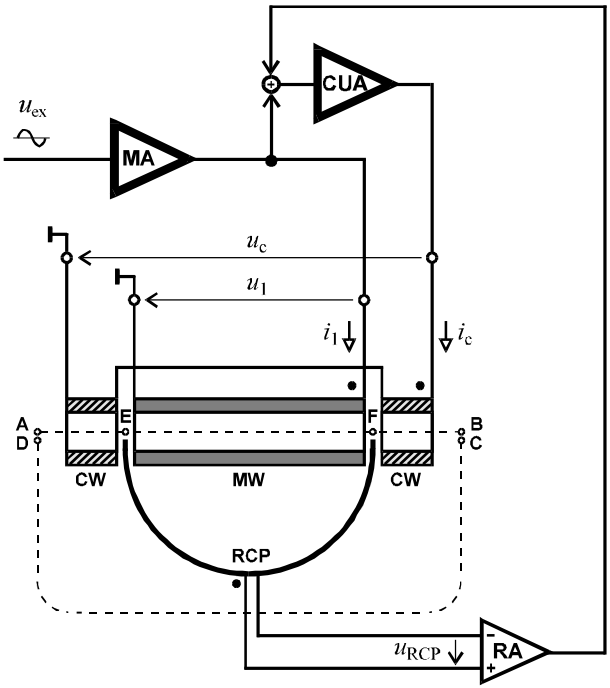

Fig. 3.1.11 MMF compensation loop with CUA

The CUA serves as a summing amplifier with unit gain. If $u_{RCP} = 0$ the magnetizing winding MW and compensation winding CW-CW are excited by the same voltage u_1. The compensation winding serves like “parallel” magnetizing section in this case. If the turn numbers N_1 and N_c are identical, both currents i_1 and i_c will be identical, too.

The MMF compensation loop (RCP – DA – CUA – CW-CW) operates also as proportional feedback with control deviation $\Delta U_m = U_{mRCP}$. However the necessary integration element is replaced by the compensation winding CW-CW at its voltage excitation from the CUA.

The MMF compensation method advatages (disadvantages):

Advantages:

- no extreme requirements on yoke quality
- simple and absolute measurement of actual physical values ($u_2(t)$, $i_1(t)$)
- no need of RCP calibration (RCP is zero indicator only)
- use possibility for on-line testing (OLT).

Disadvantage:

- feedback loop – unstability hazard.

Let´s discuse two special problems of the MMF compensation method and explain their solution at the end of this chapter.

Magnetic field homogeneity

The magnetizing current i_1 of the magnetizing windiung MW supported by the compensation current i_c of the comensation winding CW-CW generates the MMF $N_1 i_1$ distributed only along the measured region E–F if MMF drops out of the specimen measured region E–F are compensated. Although the compensation winding CW-CW serves as additional magnetizing winding (Fig. 3.1.12) supporting the magnetic field homogeneity, the actual distribution of the MMF $N_1 i_1$ along the measured region E–F is not uniform (magnetizing and compensating windings boundary effects). The generated magnetic field H is non-homogeneous.

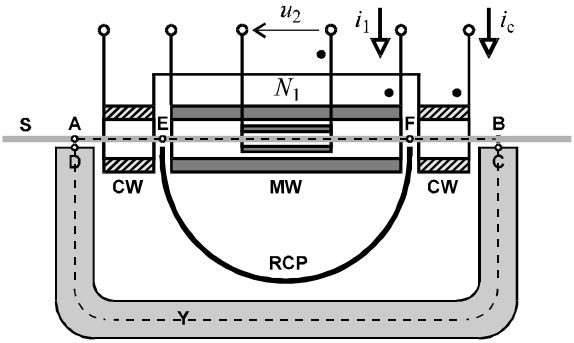

Fig. 3.1.12 Classic MMF compensation magnetizing equipment

The homogeneous magnetic field H can be considered in a relatively short region of the measured material under the central part of the magnetizing winding MW only, where the measuring voltage winding VW (N_2 turns of thin wire closely wound on the measured specimen) is placed. The VW is used for the magnetic flux density measurement (2.2.5), (2.2.6).

Due to considered homogeneity of the magnetic field H the measured region of the specimen (region between the RCP poles) can be chosen shorter, under the central part of the magnetizing winding MW only. The original magnetizing winding MW is therefore divided into three sections connected in series MW2-MW1-MW3 for this purpose. The central section of the magnetizing winding MW1 with N_{11} turns ($N_{11} < N_1$) (covering also the voltage winding VW) is enclosed by the RCP. New measured region I–J between the RCP poles is defined in this case (Fig. 3.1.13). The magnetic field in this shorter measured regin (the length of which is $l_{IJ} < l_{EF}$) is supposed to be more homogeneous.

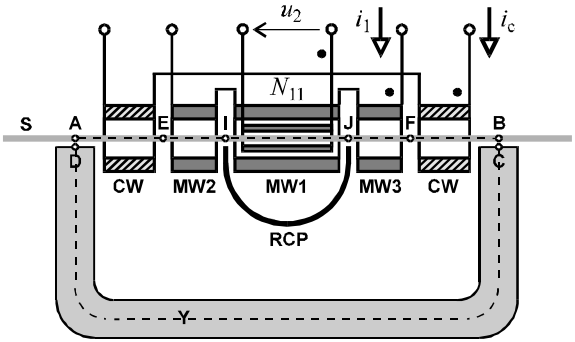

Fig. 3.1.13 Modified MMF compensation magnetizing equipment

The principle of the measurement is not changed but original parameters l_{EF} and N_1 must be substituted by l_{IJ} and N_{11}, respectively. It is valid:

$$\int_I^J H\,\mathrm{d}l \;=\; \overline{H}\,l_{IJ} \;=\; N_{11} i_1 \qquad \Rightarrow \qquad \overline{H} \;=\; \frac{N_{11} i_1}{l_{IJ}}\,, \tag{3.1.16}$$

$$p \;=\; \frac{1}{r\,l_{IJ}\,S}\,\frac{N_{11}}{N_2}\,\frac{1}{T}\int_0^T i_1\,u_2\,\mathrm{d}t\,. \tag{3.1.17}$$

The N_{11} is a turn number of the central part of the magnetizing winding only enclosed by the RCP ($N_{11} < N_1$) and $l_{IJ}\,S$ volume of the measured material part between RCP poles only.

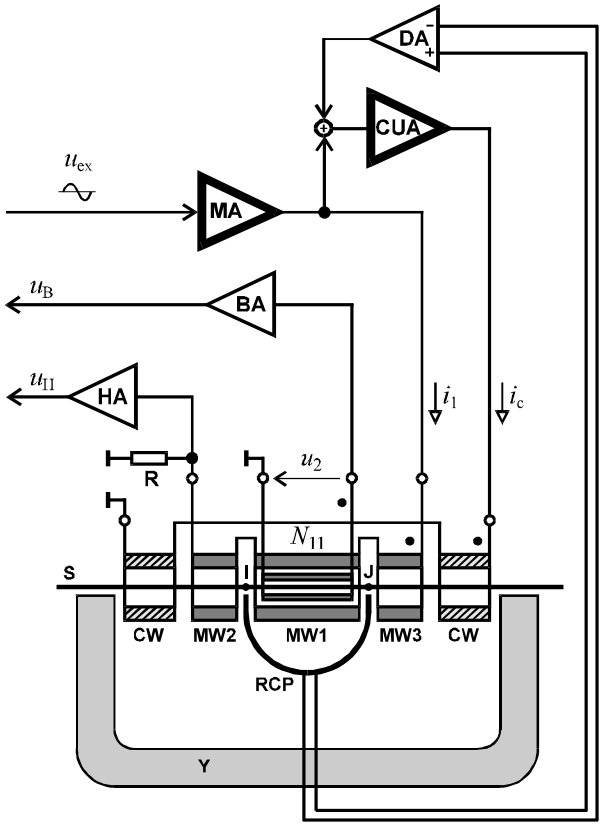

Fig. 3.1.14 Complete analog magnetizing and measuring system

MMF compensation metod accuracy

The finite gain of the compensation feedback loop causes non-zero MMF measured by RCP ($U_{mRCP} \neq 0$). This imperfection [40] creates the difference ΔH between the magnetic field strength $\overline{H}$ evaluated from (3.1.16) and the actual magnetic field strength H^* in the measured region:

$$H^* = \overline{H} - \Delta H = \frac{N_1 i_1}{l_m} - \frac{U_{mRCP}}{l_m}. \qquad (3.1.18)$$

Since the MMF U_{mRCP} is proportional to the integral of the electric voltage u_{RCP} induced in the RCP the magnetic field strength difference ΔH can be directly measured.

The magnetic field strength measurement uncertainty given by the difference ΔH has negative influence on the specific power losses p measurement uncertainty δ_p [40]:

$$p = \frac{f}{\rho}\oint H\,\mathrm{d}B = \frac{1}{\rho N_2 S}\,\frac{1}{T}\int_0^T H\,u_2\,\mathrm{d}t\,. \tag{3.1.19}$$

$$p_{\mathrm{err}} = \frac{f}{\rho}\oint \Delta H\,\mathrm{d}B = \frac{1}{\rho N_2 S}\,\frac{1}{T}\int_0^T \Delta H\,u_2\,\mathrm{d}t\,. \tag{3.1.20}$$

$$d_p = \frac{p_{\mathrm{er}}}{p}100\%\,. \tag{3.1.21}$$

At sinusoidal voltage magnetization, when the sinusoidal waveform of the induced voltage $u_2(t)$ is also supposed (due to efficient waveform correction – see next chapter):

$$u_2(t) = U_{2\mathrm{a}}\sin\left(\frac{2\pi}{T}t\right), \tag{3.1.22}$$

the specific power loss p and its error p_{err} are determined by the first harmonic component $H_1(t)$ of the $\overline{H}(t)$ and $\Delta H_1(t)$ of the $\Delta H(t)$.

$$H_1(t) = H_{1\mathrm{a}}\sin\left(\frac{2\pi}{T}t + \varphi_{H_1}\right) \tag{3.1.23}$$

$$\Delta H_1(t) = \Delta H_{1\mathrm{a}}\sin\left(\frac{2\pi}{T}t + \varphi_{\Delta H_1}\right) \tag{3.1.24}$$

$$p = \frac{1}{\rho N_2 S}\,\frac{U_{2\mathrm{a}}H_{1\mathrm{a}}}{2}\cos\left(\varphi_{H_1}\right) \tag{3.1.25}$$

$$p_{\mathrm{err}} = \frac{1}{\rho N_2 S}\,\frac{U_{2\mathrm{a}}\Delta H_{1\mathrm{a}}}{2}\cos\left(j_{\Delta H_1}\right) \tag{3.1.26}$$

The specific power loss uncertainty δ_p can be expressed by the amplitudes $H_{1\mathrm{a}}$ ($\Delta H_{1\mathrm{a}}$) and phase shifts φ_{H1} ($\varphi_{\Delta H1}$) of these components $H_1(t)$ ($\Delta H_1(t)$) toward to the sinusoidal induced voltage $u_2(t)$ [40]:

$$dp = \frac{\Delta H_{1\mathrm{a}}\cos\left(j_{\Delta H_1}\right)}{H_{1\mathrm{a}}\cos\left(j_{H_1}\right)}100\%\,. \tag{3.1.27}$$

The formula (3.1.27) shows that the power loss measurement uncertainty (caused by the imperfect MMF compensation) can be decreased (improved)

either by minimization of the first harmonic component $\Delta H_1(t)$ of the error signal U_{merr} (integrated RCP error signal u_{RCP}) or setting of the phase shift $\varphi_{\Delta H1}$ of this component to the value $\varphi_{\Delta H1} = \pi/2$.

The actual causal system for the signal processing in real time is not able to realise these ideas. It can operate properly in the periodic steady state in pseudo-real-time mode when the processed signal is delayed a time corresponding to one or more periods. The used pseudo-real-time signal processing is based on the cutting of the compensation feedback loop and creating two separate parts without the real-time signal connection: measuring and digitizing part and signal generating one [40].

The best results were found in an arrangement of the compensation loop consisting of two parallel branches (see Fig. 3.1.15). The first of these is the original analogue feedback branch (RCP – differential preamplifier DA – power amplifier CUA – compensation winding CW-CW. The second branch represents the off line operating DSP unit. This unit operates with two input signals, compensation loop error signal u_{err} (amplified u_{RCP}) and induced voltage waveform u_B ($u_B \sim u_2$). The DSP unit output signal u_{out} is added to the loop error signal on the power amplifier input.

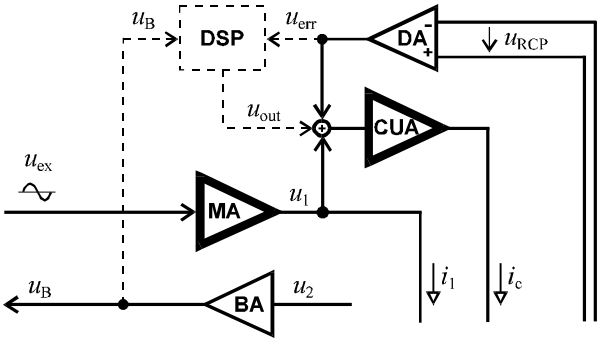

Fig. 3.1.15 MMF compensation loop digitization

The DSP unit processes the error signal u_{err} using the FFT [40] and generates. The compensation feedback contribution to the input signal of the power compensating amplifier CUA is the sum of the error signal u_{err} and the DSP unit output signal u_{out} (correction signal). Starting from zero correction, the DSP algorithm generates in the first step the sinusoidal correction signal uerr(t) and the correction signal from the previous step (the next FFT processing starts after the end of the previous step transient). After an infinite number of steps the first harmonic komponent of power amplifier exciting signal from the original analogue branch is completely

replaced by the artificial signal from the DSP unit. Then the analogue signal at the output of the differential preamplifier (corresponding to the MMF error signal) does not contain the first harmonic component.

The basic verification [40] of the presented idea was done on the compensated single sheet tester KF7 [15] (developed at the Department of Circuit Theory FEE CTU in Prague) with additional equipment. As the DSP unit was used a fixed point 16-bit TMS320C5x signal procesor with appropriate codec and filters. The specimens of grain oriented material Eo10 were measured for magnetic flux density B_a up to 1.8 T and specimens of non-oriented material Ei60 for B_a up to 1.6 T at frequency of 50 Hz. The measurement accuracy of the original analogue compensation loop and accuracy of the digitized one were measured and compared for open analog loop gain G_o 30, 24 and 18 dB. The first harmonic component suppression A_{H1} achieved by the digital signal processing, original analogue loop power loss measurement uncertainty $|\delta_{pA}|_{max}$ in comparison with the experimental digitized loop one $|\delta_{pD}|_{max}$ are presented. Measured signals are in Fig.3.1.16.

Tab. 3.1.1 MMF compensation method accuracy inrease demonstration

Material	G_0(dB)	A_{H1}(dB)	$\lvert\delta_{pA}\rvert_{max}$	$\lvert\delta_{pD}\rvert_{max}$
Eo10	30	18.5	2.8 %	0.8 %
	24	24.2	4.1 %	0.6 %
	18	29.2	6.8 %	1.0 %
Ei60	30	27.4	1.6 %	0.10 %
	24	26.9	3.1 %	0.25 %
	18	27.3	6.0 %	0.60 %

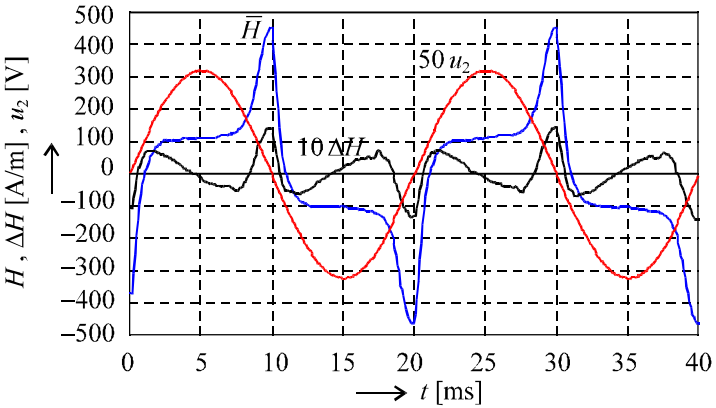

Fig. 3.1.16 Measured signals (Ei60, G_o = 24 dB, B_a = 1.5 T)

The experimental results show that using DSP system the uncertainty of the MMF compensation method can be decreased approximately 5 times for measurement of grain oriented materials and more than 10 times for non-oriented materials. This enables the MMF compensation method to be used in all kinds of precise measurements including cases of saturation [40].

The MMF compensation method became the base for the construction of PC controlled single sheet and on-line testers (compensation ferrometers) at the Czech Technical University in Prague. The analogue electronics is completed by D/A and A/D interfaces – special PC plug-in boards. These boards are able to digitally synthesize the exciting signal u_{ex} or to digitize the measured signals $u_B \sim u_2$, $u_H \sim i_1$, $u_{err} \sim u_{RCP}$. The experimental DSP system can be replaced by the bi-directional converter DADC (Fig. 3.1.17).

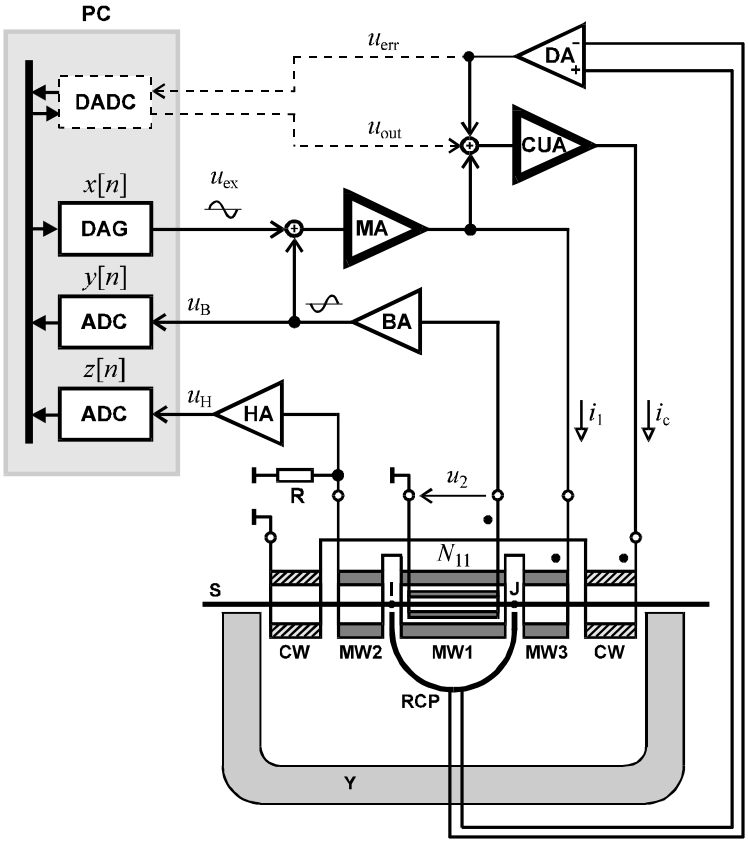

Fig. 3.1.17 PC controlled magnetizing and measuring system

3.2 Magnetic flux density waveform

For correct and exact measurement of magnetic materials parameters and for required repeatability of the measurement it is necessary to provide exactly defined magnetizing conditions in the measured material, i.e.:

- homogeneous magnetic field $H(t)$
- required magnetic flux density waveform $B(t)$.

The problem of the required magnetic flux density waveform generation at different intensities of the magnetization is discussed in this chapter.

The magnetic flux density waveform $B(t)$ is provided by the special magnetizing system (Fig. 3.2.1) [27], [28], [34], [37].

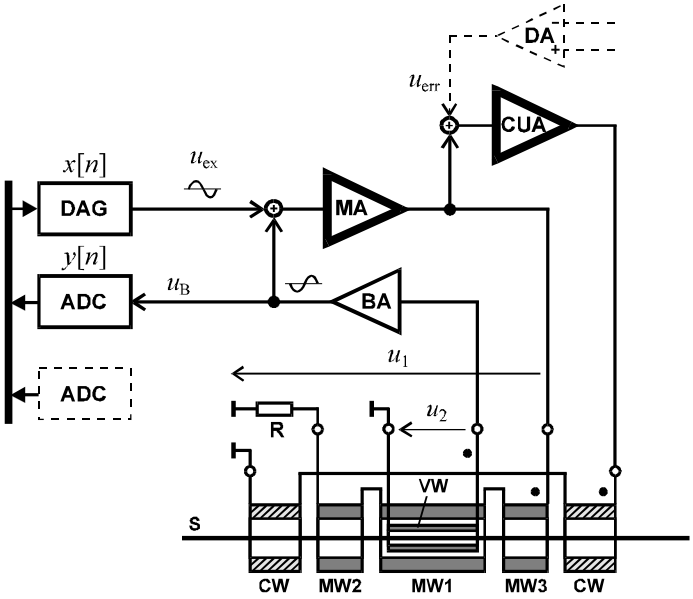

Fig. 3.2.1 Magnetizing system

The SST magnetizing system consists of three components:

- Magnetizing system base DAG – MA – MW (3 sections)
- MMF compensation loop RCP – DA – CUA – CW (2 sections)
- Magnetic flux density waveform correction feedback loops
  - MA – MW– VW – BA – MA
  - DAG – MA – MW– VW – BA – ADC – DAG.

The base of the magnetizing system (DAG – MA – MW) generates the periodical arbitrary waveform magnetizing voltage $u_1(t)$ with the variable amplitude U_{1a} and frequency f. The $u_1(t)$ waveform is digitally synthesized in the exciting signal generator DAG (special PC plug-in board). The 12-bit „samples“ of the magnetizing voltage waveform – digital prototype $x[n]$ – are calculated by the differentiation of the required magnetic flux density waveform $B_{rq}(t)$ described by the unit waveform function $f_B(t)$, and the amplitude B_{rqa}. The resulting magnetizing voltage $u_1(t)$ is given by the unit waveform function $g(t)$, and the amplitude U_{1a} (digitally controlled by the programmable gain K_{DAG} of the DAG 12-bit DA converter and the gain A_{MA} of the magnetizing amplifier MA).

$$B_{rq}(t) = B_{rqa}\, f_B(t) \tag{3.2.1}$$

$$u_1(t) = N_1 S \frac{\mathrm{d}B_{rq}}{\mathrm{d}t} = N_1 S\, B_{rqa} \frac{\mathrm{d}f_B}{\mathrm{d}t} \tag{3.2.2}$$

$$g(t) = \frac{\dfrac{\mathrm{d}f_B}{\mathrm{d}t}}{\max\left[\left|\dfrac{\mathrm{d}f_B}{\mathrm{d}t}\right|\right]} \tag{3.2.3}$$

$$x[n] = \mathrm{round}\left[\left(2^{11}-1\right)\cdot g\left(nT_s\right)\right] \tag{3.2.4}$$

$$u_1(t) = A_{MA}\, K_{DAG} \underbrace{\sum_{n=-\infty}^{\infty} x[n] \frac{\sin\left[\dfrac{p}{T_s}(t-nT_s)\right]}{\dfrac{p}{T_s}(t-nT_s)}}_{u_{ex}(t)} = U_{1a}\, g(t) \tag{3.2.5}$$

$$U_{1a} = A_{MA}\, K_{DAG}\left(2^{11}-1\right). \tag{3.2.6}$$

The T_s is a “sampling” period given by the required number of points N of one period of the digital prototype $x[n]$ ($NT_s = T = 1/f$). In the case of the sinusoidal magnetization:

$$f(t) = \sin\left(\frac{2\pi}{T}t - \frac{\pi}{2}\right) \quad \Rightarrow \quad g(t) = \sin\left(\frac{2\pi}{T}t\right) \tag{3.2.7}$$

$$x[n] = \mathrm{round}\left[\left(2^{11}-1\right)\cdot\sin\left(\frac{2\pi}{N}n\right)\right]. \tag{3.2.8}$$

The magnetizing voltage $u_1(t)$ produced by the magnetizing system according to the formula (3.2.2) does not generate the required magnetic flux density waveform $B_{rq}(t)$ (3.2.1) exactly. Due to the magnetic flux dispersion and non-zero resistance of the magnetizing winding, the actual magnetic flux density waveform $B(t)$ monitored by the induced voltage $u_2(t)$ of the voltage winding VW (respectively by its digital representation $y[n]$) :

$$u_2(t) = N_2 S \frac{\mathrm{d}B}{\mathrm{d}t} \tag{3.2.9}$$

$$y[n] = K_{\mathrm{ADC}} A_{\mathrm{BA}} u_2(nT_s), \tag{3.2.10}$$

differs from the required waveform $B_{rq}(t)$. The significant differences between the waveforms $B(t)$ and $B_{rq}(t)$ (including amplitudes B_a and B_{rqa}) are discovered at high intensities of the magnetization near saturation.

The described effect can be modelled by the non-linear dependence between the instantaneous values of the $B(t)$ and $B_{rq}(t)$ (3.2.11) determined experimentally [41–43]:

$$B(t) = B_{rq}(t) - \frac{1}{3B_m^2} B_{rq}^3(t). \tag{3.2.11}$$

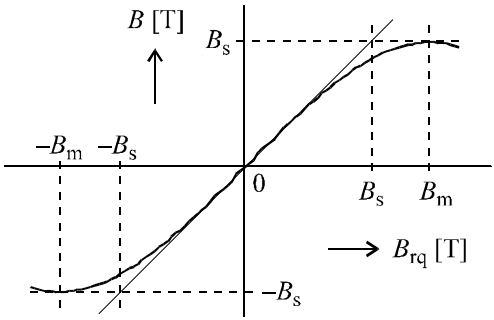

Fig. 3.2.2 Magnetic flux density distortion model

The parameter B_m (monotony limit) was determined for silicon electrical steels sheets as $B_m \approx 3$T by the experimental SST KF9a measurements at sinusoidal magnetization $f = 50$ Hz. The saturation magnetic flux density B_s is in this case:

$$B_s = \frac{2}{3} B_m \approx 2\,\mathrm{T}. \tag{3.2.12}$$

The magnetizing process demonstrating the distortion of the magnetic flux density waveform $B(t)$ at the sinusoidal magnetization up to the

saturation is shown in Fig. 3.2.3. The distortion of the magnetic flux density waveform $B(t)$ is monitored by the distortion of the induced voltage waveform $u_2(t)$ (digitized as $y[n]$) in comparison with the magnetizing voltage waveform $u_1(t)$ (given by the digital prototype $x[n]$).

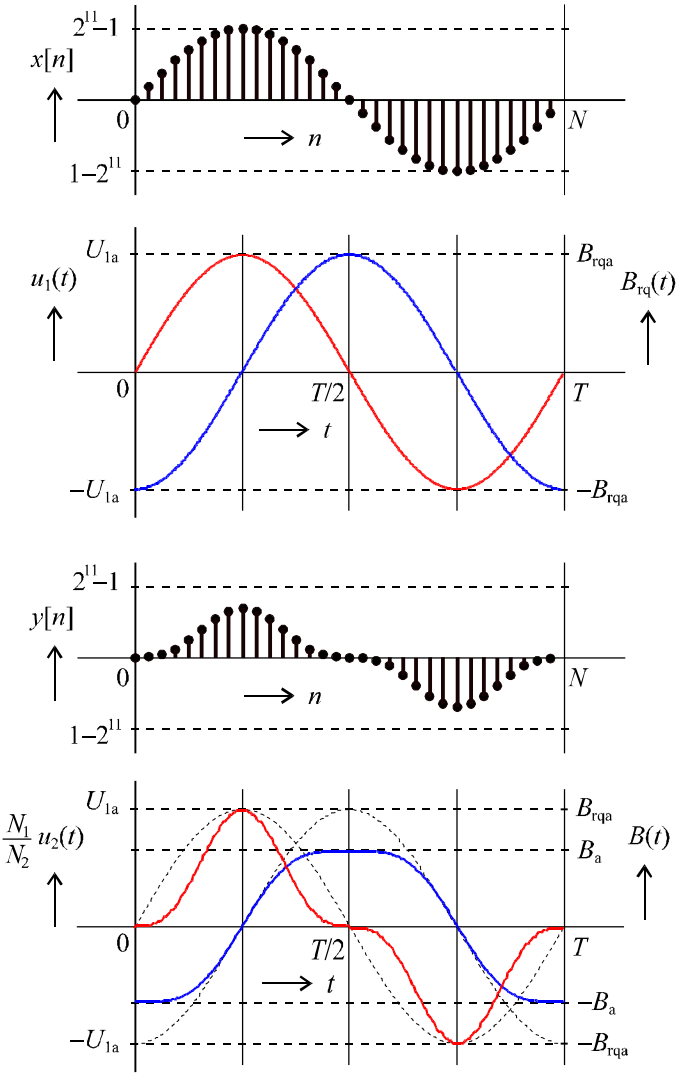

Fig. 3.2.3 Magnetic flux density and induced voltage distortion

3.2.1 Analogue correction

The distortion of the induced voltage $u_2(t)$ monitoring the non-linear distortion of the actual waveform $B(t)$ can be also modeled by the additional spurious signal $\Delta u(t)$ actuating at the magnetizing winding MW (Fig. 3.2.4).

The analog correction feedback loop MA – MW – VW – BA is a classic negative feedback excited by the analog voltage $u_{ex}(t)$ the waveform of which is determined by the magnetizing voltage digital prototype $x[n]$ stored in the memory of the generator DAG .

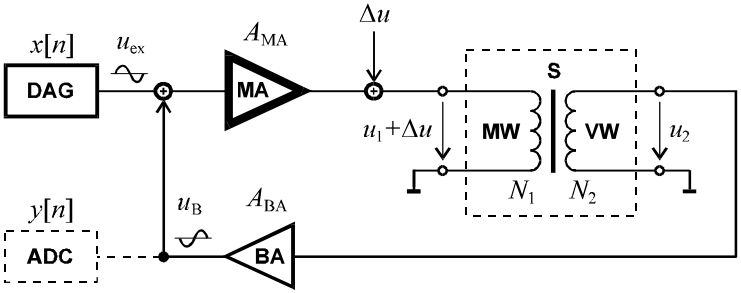

Fig. 3.2.4 Analog correction feedback loop

If the correction feedback loop is disconnected, it is valid:

$$u_2(t) = \underbrace{A_{MA}\frac{N_2}{N_1}u_{ex}(t)}_{s_2(t)} + \underbrace{\frac{N_2}{N_1}\Delta u(t)}_{n_2(t)}. \qquad (3.2.13)$$

The distorted induced voltage $u_2(t)$ consists of two components – useful signal $s_2(t)$ and distorting "noise" $n_2(t)$ (model in Fig. 3.2.4 is linear). Their magnitudes define the induced voltage signal noise ratio SNR:

$$SNR = \frac{\max\left[|\, s_2(t)\,|\right]}{\max\left[|\, n_2(t)\,|\right]} = A_{MA}\frac{\max\left[|\, u_{ex}(t)\,|\right]}{\max\left[|\, \Delta u(t)\,|\right]}. \qquad (3.2.14)$$

If the correction feedback loop is connected, both components are generally decreased by the negative feedback ($s_2^*(t)$, $n_2^*(t)$):

$$u_2(t) = \underbrace{\frac{A_{MA}\frac{N_2}{N_1}}{1-A_{BA}A_{MA}\frac{N_2}{N_1}}u_{ex}(t)}_{s_2^*(t)} + \underbrace{\frac{\frac{N_2}{N_1}}{1-A_{BA}A_{MA}\frac{N_2}{N_1}}\Delta u^*(t)}_{n_2^*(t)}. \qquad (3.2.15)$$

The induced voltage signal noise ratio SNR^* is in this case:

$$SNR^* = \frac{\max\{|s_2^*(t)|\}}{\max\{|n_2^*(t)|\}} = A_{MA}\frac{\max\{|u_{ex}(t)|\}}{\max\{|\Delta u^*(t)|\}}. \qquad (3.2.16)$$

Since the spurious signal $\Delta u^*(t)$ at given constant level of the exciting signal $u_{ex}(t)$ is decreased by the negative feedback in comparison with $\Delta u(t)$, the SNR^* (3.2.16) is increased in comparison with SNR (3.2.14).
If very strong negative feedback was applied:

$$|A_{MA}| \to \infty \qquad (3.2.17)$$

$$u_2(t) \to -\frac{1}{A_{BA}}u_{ex}(t) \qquad (3.2.18)$$

$$SNR^* \to \infty, \qquad (3.2.19)$$

the distortion of the induced voltage waveform $u_2(t)$ (non-linear distortion of the magnetic flux density waveform $B(t)$) would be perfectly corrected.

3.2.2 Digital correction

The magnetic flux density waveform $B(t)$ digital/analog correction feedback loop DAG – MA – MW – VW – BA – ADC – DAG is a special PC controlled negative feedback (Fig. 3.2.5) where the magnetizing voltage waveform $u_1(t)$ can be adaptively digitally corrected by the correction of its digital prototype $x[n]$ to find the required waveform $B(t) = B_{rq}(t)$.

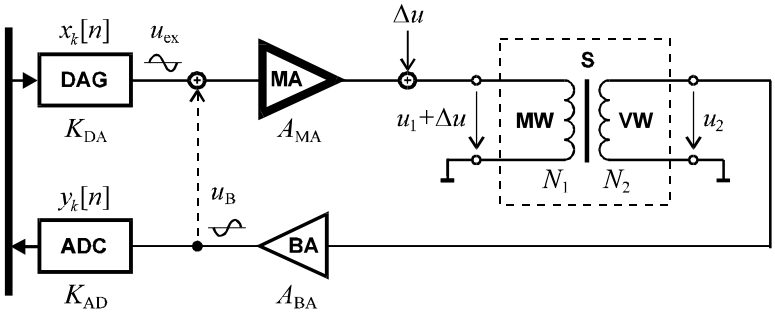

Fig. 3.2.5 Digital correction feedback loop

The digital prototype $x[n]$ (3.2.4) is replaced by the 12-bit variable digital exciting signal $x_k[n]$ with constant amplitude $(2^{11} - 1)$ the waveform of which is step by step recalculated in the convergent correction iteration process (k = 0, 1, 2, …). The main part of the correction algorithm is expressed in several formulas [29], [30], [35], [38]:

1. Initialization:

$$k = 0 \tag{3.2.20}$$

$$x_k[n] = x[n] \tag{3.2.21}$$

2. Digital exciting signal amplitude normalization:

$$X_{\mathrm{a},k} = \max\left[\left|\, x_k[n] \right|\right] \tag{3.2.22}$$

$$x_k[n] = \mathrm{round}\left[\frac{2^{11}-1}{X_{\mathrm{a},k}}\, x_k[n]\right] \tag{3.2.23}$$

$$X_{\mathrm{a},k} = 2^{11}-1 \tag{3.2.24}$$

3. Digital exciting signal waveform factor determination:

$$X_{\mathrm{s},k} = X_{\mathrm{sar},k} = \frac{1}{N}\sum_{n=0}^{N-1}\left|\, x_k[n] \,\right| \tag{3.2.25}$$

$$k_{\mathrm{p},k} = \frac{X_{\mathrm{s},k}}{X_{\mathrm{a},k}} = \frac{X_{\mathrm{s},k}}{2^{11}-1} \tag{3.2.26}$$

4. DAG 12-bit DA converter gain programming:

$$K_{\mathrm{DAG},k} = \frac{4\, f N_1 S B_{\mathrm{rqa}}}{k_{\mathrm{p},k}\, A_{\mathrm{MA}}\left(2^{11}-1\right)} \tag{3.2.27}$$

5. Response measurement:

$$x_k[n] \quad \Rightarrow \quad y_k[n] \tag{3.2.28}$$

6. Data processing and correction process:

$$Y_{\mathrm{a},k} = \max\left[\left|\, y_k[n] \right|\right] \tag{3.2.29}$$

$$y_k[n] = \frac{X_{\mathrm{a},k}}{Y_{\mathrm{a},k}}\, y_k[n] = \frac{2^{11}-1}{Y_{\mathrm{a},k}}\, y_k[n] \tag{3.2.30}$$

$$c_k[n] = x[n] - y_k[n] \tag{3.2.31}$$

$$d = \frac{1}{2^{11}-1}\sqrt{\frac{1}{N}\sum_{n=0}^{N-1} c_k^2[n]} \tag{3.2.32}$$

$$\text{if } d < d_{\mathrm{a}}: \quad \text{stop}$$

$$\text{else}: \quad x_{k+1}[n] = x_k[n] + c_k[n] \tag{3.2.33}$$

$$k = k+1 \tag{3.2.34}$$

7. Next iteration cycle – jump to 2.

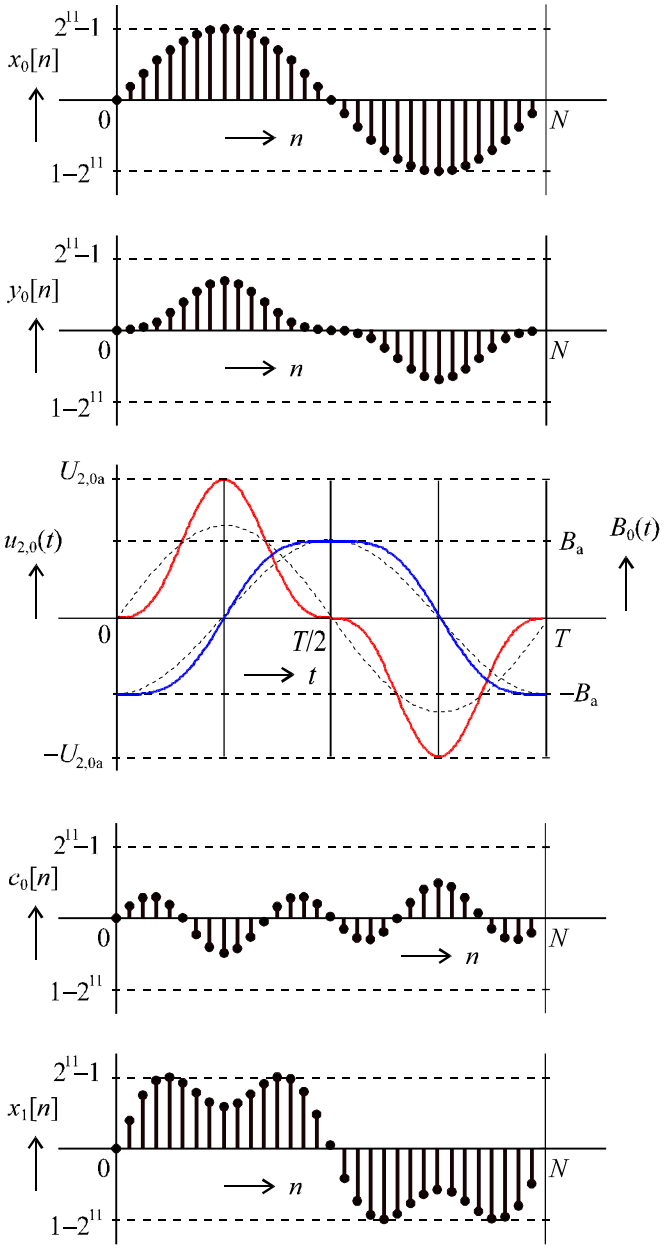

Fig. 3.2.6 Correction process ($k = 0$)

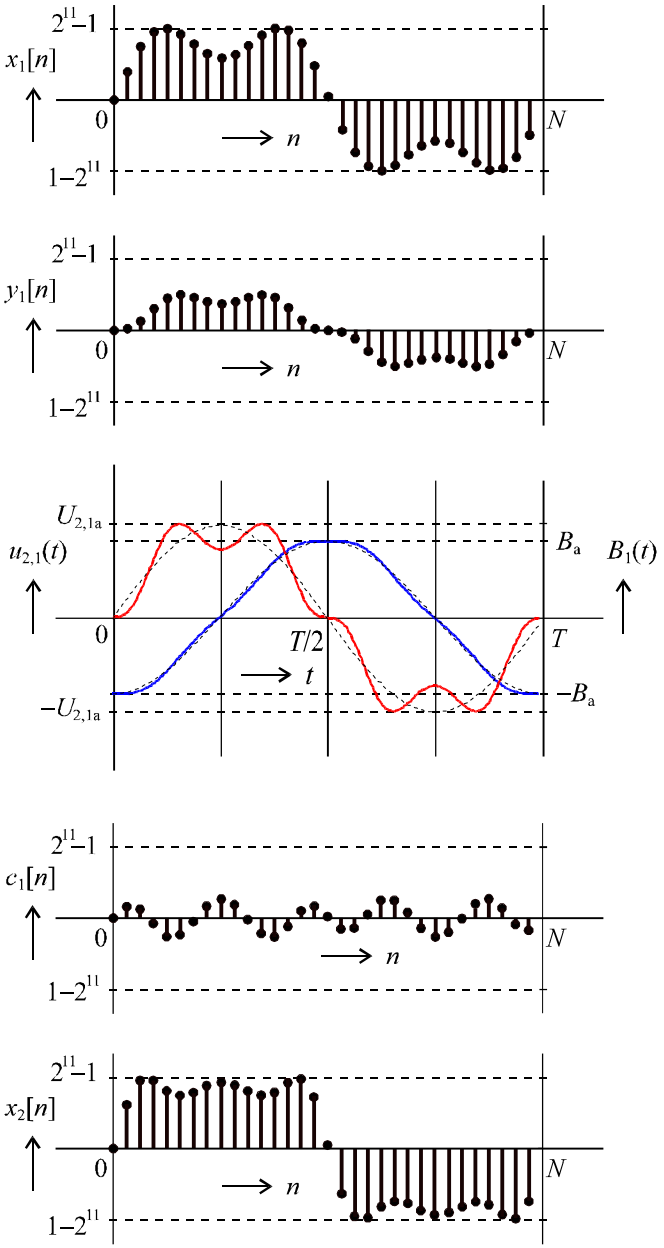

Fig. 3.2.7 Correction process (k = 1)

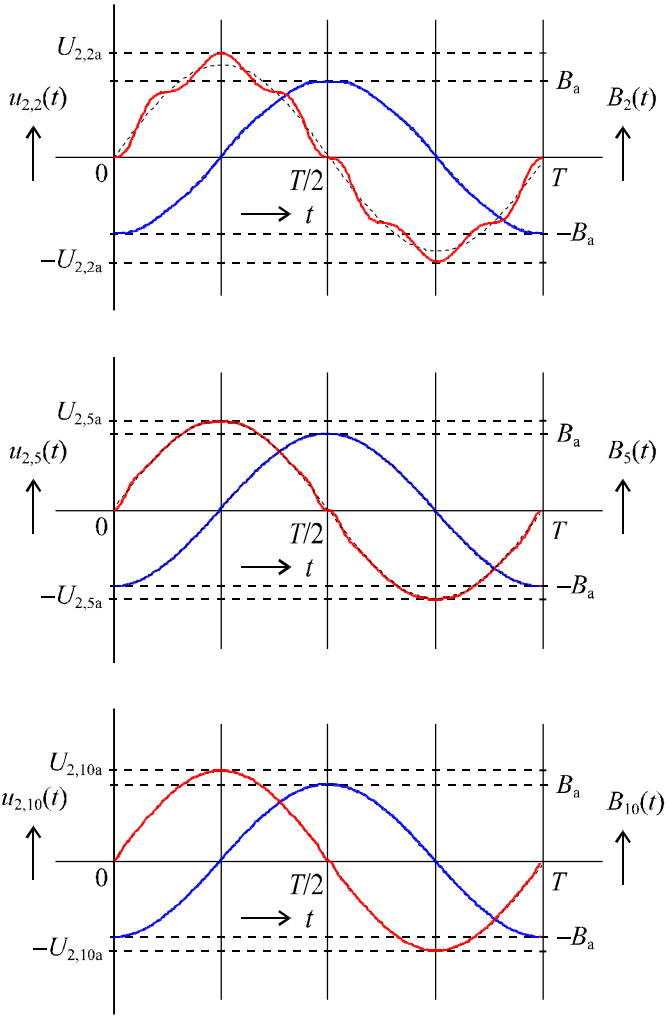

Fig. 3.2.8 Results of correction process (k = 2, 5, 10)

The described correction process for required magnetic flux density amplitude B_{rqa} (operating point) changes only the waveform of the magnetic flux density $B(t)$ - not its amplitude. Therefore the correction algorithm must control the magnetizing voltage waveform $u_1(t)$ with respect to the constant average value within a half-period U_{2s} of the induced voltage $u_2(t)$ [29], [30], [35], [38], [41–43], see eqn. (2.2.8) :

$$U_{1s} = 4 f N_1 S B_{rqa} \tag{3.2.35}$$

$$B_a = \frac{U_{2s}}{4 f N_2 S} . \tag{3.2.36}$$

The magnetic flux density waveform correction ability of the described magnetizing system was verified in practice by the measurement on new singe sheet testers KF8 and KF9a developed at the Department of Circiut Theory of the FEE CTU in Prague. The form factors of the induced voltage u_2 measured at the sinusoidal voltage magnetization of electrical steel sheets Eo10 at frequency 50 Hz for magnetic flux density amplitudes 1.0 T, 1.5 T, 1.7 T are in Tab. 3.2.1 (A – no correction, B – analog correction, C – digital correcton (3 iteration steps)). The measured form factors are compared with the form factor of the ideal sinusoidal waveform (1.1107).

Tab. 3.2.1 Induced voltage form factors at sinusoidal voltage magnetization

B_a (T)	Form factors		
	A	B	C
1.0	1.1131	1.1113	1.1109
1.5	1.1218	1.1126	1.1115
1.7	1.1954	1.1295	1.1156

3.3 Automated measurements

A special computer-controlled single sheet testers based on the compensation method are used for the automated measurements of basic characteristics of soft magnetic materials at AC magnetization:

- *amplitude magnetizing characteristic* – dependence of the magnetic flux density amplitude B_a on magnetic field strength amplitude H_a

$$B_a = f_1(H_a) \tag{3.3.1}$$

- dependence of *specific power losses* p on the magnetic flux density amplitude B_a

$$p = f_2(B_a) . \tag{3.3.2}$$

These characteristics are measured in several operating points defined by the material standard. The computer controlled measurements brings problems if the dependence between the controlled magnetic values to be set up (H_a or B_a amplitudes) and the controlling value is strong non-linear. The block diagram of the computer-controlled measurement is in Fig. 3.3.1.

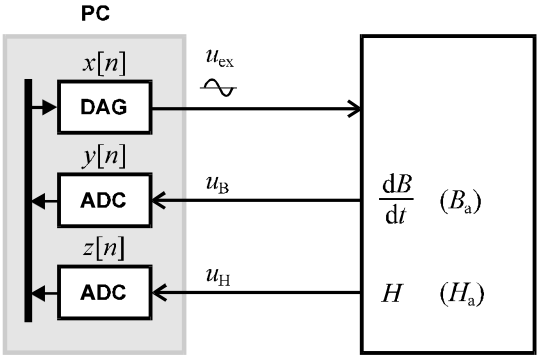

Fig. 3.3.1 Computer controlled measurement

The amplitudes H_a and B_a in the measured material are controlled by the digital signal U from the PC through the digitally controlled gain $K_{DAG}(U)$ of the exciting signal generator DAG:

$$K_{DAG}(U) = \frac{10}{2^{12}} \cdot \frac{U}{2^{15}}. \tag{3.3.3}$$

Due to the voltage excitation of the magnetizing equipment (yoke) the B_a dependence on the digital control signal U is linear (or weakly non-linear), while the H_a one is strongly non-linear (given by the strong non-linearity of the magnetizing characteristic $B_a = f_1(H_a)$) [18], [20], [25], [26], [33], [36].

$$B_a = K_1 U = b(U) \tag{3.3.4}$$

$$H_a = f_1^{-1}(B_a) = f_1^{-1}[b(U)] = h(U) \tag{3.3.5}$$

The main problem of the computer controlled measuring process consists in the reliable, quick and exact setup of all required points of the measured characteristics (required values H_{ar} and B_{ar}, respectively) defined by the material standard. The required accuracy of the H_{ar} setup is 1 % and the B_{ar} one 0.1 %. The algorithm of the H_{ar} and B_{ar} setup depends on the character of the dependences $H_a = h(U)$ and $B_a = b(U)$, respectively.

A convenient numerical method based on a iteration rule R has to be used for the H_{ar} setup in all measured points (H_{ar}) of the magnetization characteristic $B_a = f_1(H_a)$ [20], [25], [26]:

$$U_{k+1} = R\{U_k, H_{a,k}, H_{ar}\} = R\{U_k, h(U_k), H_{ar}\}, \tag{3.3.6}$$

where U_k and U_{k+1} are the values of the exciting signal U in last and next iteration cycle, respectively, $H_{a,k}$ the value of H_a in last iteration cycle and

H_{ar} the required value of the H_a. The most important properties of numerical methods are:

- reliability of convergence
- high speed of convergence.

The regula falsi method (or "discrete" Newton's method) is the convenient numerical method experimentally chosen for this purpose [20], [25]:

$$U_{k+1} = U_k + \frac{U_0 - U_k}{H_{a,0} - H_{a,k}}\left(H_{ar} - H_{a,k}\right). \qquad (3.3.7)$$

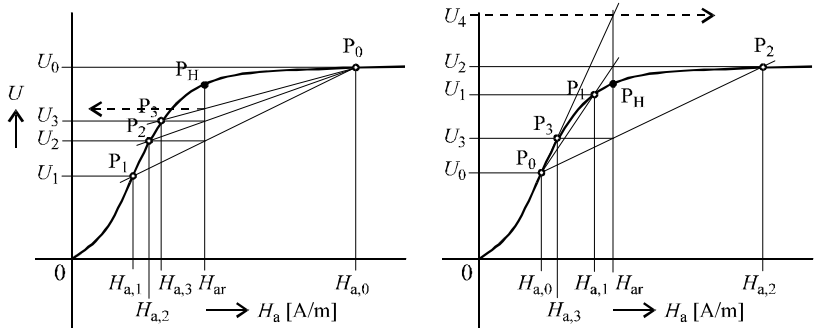

Fig. 3.3.2 The convergent and divergent regula~falsi iteration

The setup process using the regula~falsi method reliably converges if the required set up value H_{ar} is inside the interval (H_{a1} , H_{a0}) (point P_H is between points P_1 and P_0). The limits of this interval are last two H_a values set up before the iteration. If the required setup value H_{ar} is outside this interval the setup process could be divergent (Fig. 3.3.2).

For the reliability of the convergence it is necessary to use not only the convenient numerical method but also the special measuring procedure, that consists of:

1. magnetiziation of the material up to the saturation
2. high speed of convergent measurement of the $B_a = f_1(H_a)$ and $p = f_2(B_a)$ in required points from the largest values H_{ar} and B_{ar} , respectively, to zero ones
3. $B(t)$ waveform check/correction in all measured points.

The exciting voltage U controls the gradual increse of the H_a and B_a in material during the magnetization. It increases gradually step by step ΔU until $H_a > H_{a,max}$ (10000 A/m for silicon steels). The prospective material

remanence is suppressed by this way. The increase of the U is finished and the start point of the measurement P_0 is defined:

$$\text{if } H_a > H_{a,max}: \quad P_0 \equiv \left[U_0 = U,\ H_{a,0} = h(U_0),\ B_{a,0} = b(U_0) \right]. \qquad (3.3.8)$$

The relations $H_{a,0} > H_{ar}$ and $B_{a,0} > B_{ar}$ are true for all required values H_{ar} and B_{ar} to be set up during the following measurement. The non-linear distortion of the $B(t)$ waveform is not serious at this measuring phase.

The measurement of the $B_a = f_1(H_a)$ and $p = f_2(B_a)$ in all required points P_H and P_B, respectively, is the second phase of the measuring procedure.

$$P_H \equiv \left[U,\ H_{ar} = h(U),\ B_a = f_1(H_{ar}) \right] \qquad (3.3.9)$$

$$P_B \equiv \left[U,\ B_{ar} = b(U),\ p = f_2(B_{ar}) \right]. \qquad (3.3.10)$$

Both characteristics are measured simultaneously from the largest values H_{ar} and B_{ar}, respectively, down to zero ones.

The exciting voltage U decreases gradually step by step ΔU from the U_0 value and values H_a and B_a approach to the required values H_{ar} and B_{ar}, respectively. This approach is finished and the point P_1 is defined:

$$\text{if } (H_a \le H_{ar}) \vee (B_a \le B_{ar}):$$
$$P_1 \equiv \left[U_1 = U,\ H_{a,1} = h(U_1),\ B_{a,1} = b(U_1) \right]. \qquad (3.3.11)$$

The H_{ar} or B_{ar} setup process starts after the approach. In the case of H_{ar} setup process the numerical iteration method has to be used. The set up point P_H is in the region between the points P_0 and P_1 of the $H_a = h(U)$ dependence and the H_{ar} setup process reliably converges (Fig. 3.3.2).

The H_{ar} or B_{ar} setup process is finished if the value H_{ar} or B_{ar} set up with required accuracy or if the limited number of the iteration cycles (H_{ar} setup process) is used up. When the required operating point is set (H_{ar} or B_{ar}), the reached amplitude B_a is stored and $B(t)$ waveform correction process starts at this B_a amplitude (see chapter 3.2). If the required $B(t)$ waveform is found with required accuracy the correction process and the measurement of one point of the $B_a = f_1(H_a)$ or $p = f_2(B_a)$ is finished.

The described measurement including the approach, setup and correction processes is repeated until the measurement of the $B_a = f_1(H_a)$ and $p = f_2(B_a)$, respectively, in all required points P_H and P_B is over.

The reliability of convergence is one of two problems of the H_{ar} setup process. The second one is the speed of the convergence expressed by relatively great number of iteration cycles (k_i). The great number of iteration

cycles for the H_{ar} setup is necessary if the set up point P_H is in the strong non-linear region of the $H_a = h(U)$ and the points P_0 and P_1 are too distant.

If the modified version of the regula~falsi method is used (discrete Newton's iteration method) the point P_0 is not fixed. After every approach step (ΔU decrease of U) the current H_a and B_a values are compared with the H_{ar} and B_{ar} ones and point P_0 eventually redefined [20], [25], [26]:

$$\text{if } (H_a > H_{ar}) \wedge (B_a > B_{ar}):$$
$$P_0 \equiv \left[U_0 = U,\ H_{a,0} = H_a,\ B_{a,0} = B_a \right]. \qquad (3.3.12)$$

The speed of the H_{ar} setup process is higher in this case (the great number of iteration cycles is reduced). The reason of this improvement consists in the reduction of the points P_0, P_H, P_1 distantace. However this improvement is not too significant if the H_{ar} setup process is applied on the points P_H placing in the strong non-linear region of the $H_a = h(U)$. Due to the strong non-linearity it is necessary to use a quality different method for more significant H_{ar} setup process improvement.

The basic idea how to make the speed of the iteration process higher (how to reduce the great number of the iteration cycles) consists in the transformation G of the non-linear dependence $H_a = h(U)$:

$$G\{ H_a \} = G\{ h(U) \} \qquad (3.3.13)$$

and the application of the iteration formula (3.3.6) on the transformed dependence (3.3.13) instead of the (3.3.5) one:

$$U_{k+1} = R\left\{ U_k, G\{ h(U_k) \}, G\{ H_{ar} \} \right\}. \qquad (3.3.14)$$

If a convenient transformation G has the linearisation effect on the $h(U)$ i.e. if the transformation G transforms the strong non-linear dependence $h(U)$ to the "not so much non-linear" one $G\{h(U)\}$ the speed of the iteration process (3.3.14) will be higher [20], [25], [26].

The transformation G derived as a function modelling the magnetizing characteristic $B_a = f_1(H_a)$ would be the most convenient one:

$$G_{ideal} = f_1. \qquad (3.3.15)$$

In this ideal case the strong "non-linear" H_{ar} setup process would be transformed to the relatively "linear" B_{ar} one:

$$G_{ideal}\{ h(U) \} = f_1\{ h(U) \} = f_1\left\{ f_1^{-1}[b(U)] \right\} = b(U) \qquad (3.3.16)$$

$$U_{k+1} = R\left\{ U_k, b(U_k), G_{ideal}\{ H_{ar} \} \right\}. \qquad (3.3.17)$$

In actual cases it is impossible to determined the ideal transformation G_{ideal} because neither the dependence (3.3.4) nor (3.3.5) (nor magnetization characteristic $B_a = f_1(H_a)$) is exactly known before the measurement. It is possible to determine the actual transformation G from the approximations of the dependences (3.3.4), (3.3.5) (or $B_a = f_1(H_a)$) in several points randomly set up during the magnetization of the material up to saturation or from the points P_0 and P_1 determined before every iteration process. The convenient approximations are logarithm function, Kneppo´s function and exponential function [11], [20], [24], [25], [26].

The designed algorithm for the automated measurement of the characteristics $B_a = f_1(H_a)$ and $p = f_2(B_a)$ was verified in the control program of the single sheet tester KF7 and KF9a. Three influences on the reliability and speed of the measurement were investigated in the control algorithm:

- influence of the exciting voltace step value ΔU on the saturation process speed (number of steps k_0), approach process speed (k_1) and measurement finish speed (k_2) and on the initial conditions for the iteration process. Two values ΔU_1 and ΔU_2 were tested
  - $\Delta B_{a1} = b(\Delta U_1) = 0.1$ T
  - $\Delta B_{a2} = b(\Delta U_2) = 0.3$ T
- influence of two numerical methods on the iteration process speed (measured by the number of iteration steps k_i)
  - standard regula~falsi method
  - “discrete” Newton's method
- influence of the transformations G on the iteration process speed (k_i)
  - identity $G\{H_a\} = H_a$
  - logarithm function $G\{H_a\} = A \log_E(kH_a + 1)$
  - Kneppo's function $G\{H_a\} = A^{(k - 1/H_a)}$
  - exponential function $G\{H_a\} = A(1 - e^{-kH_a})$

The measured results [26] are in Tab. 3.3.1 – 3.3.3. The reduction of the step ΔB_a makes proportionally lower the speeds of saturation, approach and measurement finish processes (k_0, k_1 and k_2) and makes better initial conditions for the iteration process (k_i). Higher iteration process speed does not compensate the lower speeds of other processes. That's why greater step $\Delta B_a = b(\Delta U) = 0.3$ T is used for the measurement (see Tab. 3.3.1).

The acceleration of the iteration process was reached using the “discrete” Newton's method (Tab. 3.3.2). Significantly good results were reached by the “discrete” Newton's method in combination with non-linear

transformations. The best transformation is the exponential function with the parameter $A = K_1$ and the logarithm function with the base $E = 1000$ (Tab. 3.3.3). Very good results gives the Kneppo's function in the rise region of the magnetizing characteristic (for $H_{ar} = 30$ A/m). The Kneppo's function is impossible to use near the origin [26].

Tab. 3.3.1 Regula-falsi method / Identity (no transformation)

H_{ar} [A/m]	B_a [T]	B_{ar} [T]	p [W/kg]	$\Delta B_a = 0.1$ T				$\Delta B_a = 0.3$ T			
				k_0	k_1	k_i	k_2	k_0	k_1	k_i	k_2
				39				14			
1000	1.813				21	6			9	13	
800	1.794				1	5			1	17	
		1.700	1.528		4	1			2	1	
		1.500	1.035		2	1			1	1	
30	1.305				3	1			1	20	
		1.000	0.445		2	1			1	1	
							11				4

Tab. 3.3.2 Identity (no transformation)

H_{ar} [A/m]	B_a [T]	B_{ar} [T]	p [W/kg]	$\Delta B_a = 0.3$ T	
				regula falsi	Newton
				k_i	k_i
1000	1.811			13	5
800	1.793			17	6
		1.700	1.546	1	1
		1.500	1.035	1	1
30	1.227			20	20
		1.000	0.447	1	1

Tab. 3.3.3 Newton's method / transformations

H_{ar} [A/m]	B_a [T]	B_{ar} [T]	p [W/kg]	$\Delta B_a = 0.3$ T		
				$\log_{1000}$	Kneppo	exp
				k_i	k_i	k_i
1000	1.812			3	6	4
800	1.794			3	8	4
		1.700	1.545	1	1	1
		1.500	1.033	1	1	1
30	1.298			9	3	5
		1.000	0.446	1	1	1

4. COMPENSATION FERROMETERS

The successful resolution of presented problems gives possibilities for the development and construction of special computer-controlled single sheet and on-line testers for the laboratory and industrial use. Since 1989 the series of unique PC controlled measuring systems – compensation ferrometers – for the automated measurement of soft magnetic materials parameters at AC magnetization have been developed at the Department of Circuit Theory of the FEE CTU with the significant author´s participation.

Tab. 4.0.1 Computer controlled compensation ferrometers

ferrometer	control unit	user
KF5	8-bit	FEE CTU, VÚHŽ
KF7	PC	FEE CTU
KF7a	PC	VÚHŽ
KF7b	PC	VPFM
KF8	PC	FEE CTU
KF9	PC	VPFM
KF9a	PC	FEE CTU

Fig. 4.0.1 Ferrometer KF9 / KF9a development at FEE CTU

Some of these systems are used in the industrial practice in Rolling Works Frýdek-Místek (VPFM) for on-line quality check of the producted silicon electrical steel sheets, other of them were developed for Research Institute of Ferrous Metallurgy (VÚHŽ) in Dobrá for exact laboratory measurements. Most of designed systems [3], [4], [15] are used for the research of new measuring methods and systems at the FEE CTU in Prague.

The development of the measuring systems (ferrometers KF9/KF9a) at the FEE CTU in Prague and the KF9 installation in the Rolling Works Frýdek-Místek (VPFM) are in Fig. 4.0.1, Fig.4.0.2 ([28], [34], [37]).

Fig. 4.0.2 Ferrometer KF9 installation in the VPFM

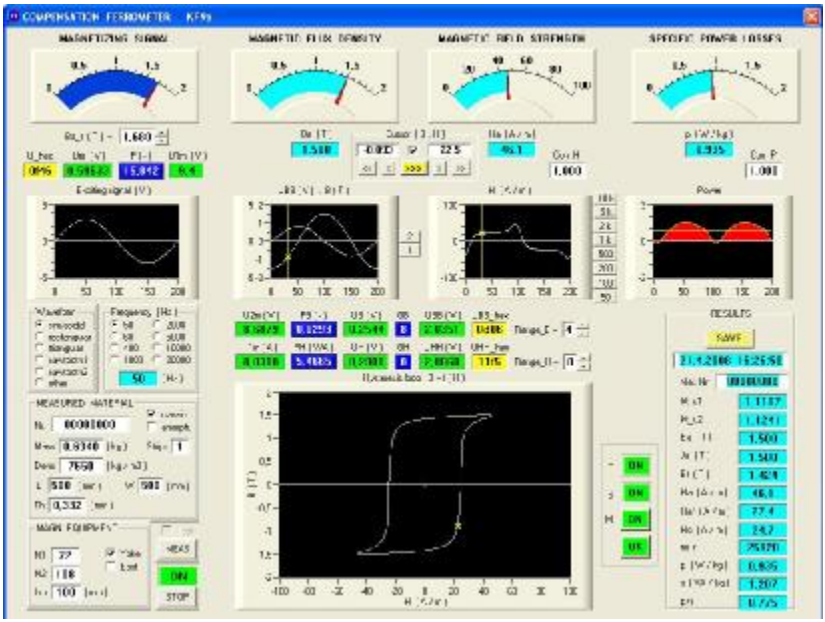

Fig. 4.0.3 Ferrometer KF9 / KF9a control software dialogue window

5. CONCLUSION

The basic specific problems of the open specimen measurements of soft magnetic materials parameters at AC magnetization were pointed out and discussed in this lecture. The possible solutions of these problems were shown and confirmed by the measurements on actual measuring system realized at the Department of Circuit Theory of the Faculty of Electrical Engineering of the Czech Technical University in Prague. The positive results were used for the realization of special measuring systems for both laboratory and industrial use.

ACKNOWLEDGEMENTS

The author thanks to his teachers Prof. Ing. Milan Mikulec, DrSc. and Prof. Ing. Václav Havlíček, CSc. for their professional leading, training and unselfish experience sharing in the field of magnetism and magnetic measurements at the beginning of his scientific career.

The author thanks to named colleagues and to other ones, who have participated in the works on many particular problems of soft magnetic materials measurements, specified in the cited references.

The research of new methods and systems for the measurement of soft magnetic materials properties at AC magnetization, performed at the Department of Circuit Theory at the Faculty of Electrical Engineering of the Czech Technical University in Prague (CTU), has be supported by grants: CTU grant No. 8047 (1991-93), GACR grant No. 102/93/1197 (1993-95), GACR grant No. 102/96/1251 (1996-98), GACR grant No. 102/01/1335 (2001-03). At present it is supported by the „A“ cathegory research program No. MSM 6840770015 sponsored by the Ministry of Education, Youth and Sports of the Czech Republic (2005-11).

REFERENCES

[1] BECKLEY, P. – PORTER, C. H. – SNELL, D., Journal of Magnetism and Magnetic Materials, 26, 1982, pp. 168 -175.

[2] HAVLÍČEK, V. – ZEMÁNEK, I., Journal of Magnetism and Magnetic Materials, 133, 1994, pp. 399 -401.

[3] HAVLÍČEK, V. – ZEMÁNEK, I., Proc. of the Czech-Polish-Hungarian Workshop on Circuit Theory and Application, Prague 1989, pp. 32-36.

[4] HAVLÍČEK, V. – ZEMÁNEK, I., Acta politechnica - Práce ČVUT v Praze, 12 ((III,3)), 1989, s. 41-49.

[5] HAVLÍČEK, V. – DRAXLER, K. – MIKULEC, M. – KAŠPAR, P. – RIPKA, P., Proccedings of the CTU Workshop 93, Prague 1993, s. 147.

[6] HAVLÍČEK, V. – MIKULEC, M., Physica Scripta, 39, 1989, p. 513.

[7] HAVLÍČEK, V. – MIKULEC, M., Proccedings of the Soft Magnetic Materials 8 (SMM 8) Conference, Bad Gastein 1987, pp. 99-100.

[8] HAVLÍČEK, V. – MIKULEC, M. – UHLÍŘ, P. – ZEMÁNEK, I., Proceedings of the CTU Workshop 92, Prague 1992, s. 115-116.

[9] MIKULEC, M., Proccedings of the Soft Magnetic Materials 3 (SMM 3) Conference, 1977, pp. 669-670 Part 2.

[10] MIKULEC, M., Vyšetřování magnetických vlastností elektrotechnických plechů. [Doktorská disertační práce], ČVUT FEL, 1988.

[11] ZEMÁNEK, I., Proccedings of the CTU Workshop 94, Prague 1994, pp. 211-212.

[12] ZEMÁNEK, I., Slaboproudý obzor (Electronic Horizon), 53, 1992, (5-6), s. 107-108.

[13] ZEMÁNEK, I., Journal of Electrical Engineering 45, No.8/S (1994), pp. 55-57.

[14] ZEMÁNEK, I., Proccedings of the Hungarian-Czech-Polish Workshop on Circuit Theory and Application, Budapest 1991, pp. 69-72.

[15] ZEMÁNEK, I., Proc. of the Polish-Czech-Hungarian Workshop on Circuit Theory and Application, Kiry (Poland) 1992, pp. 65-69.

[16] ZEMÁNEK, I., Proccedings of the Czech-Polish-Hungarian Workshop on Circuit Theory and Application, Prague 1993, pp. 125-130.

[17] ZEMÁNEK, I., Sborník Celostátního semináře kateder teoretické a experimentální elektrotechniky, VŠSE Plzeň, Cheb 1991, s. 32-34 (III).

[18] ZEMÁNEK, I., Proceedings of the 2nd Japanese-Czech-Slovak Joint Seminar on Applied Electromagnetics in Materials, Kyoto (Japan) 1994, pp. 202-205.

[19] ZEMÁNEK, I., Proccedings of the Czech-Polish-Hungarian Workshop on Circuit Theory and Application, Budapest 1987, pp. 119-124.

[20] ZEMÁNEK, I., Journal of Japan Society of Applied Electromagnetics, special issue Applied Electromagnetics in Materials (1995), Tokyo 1995, pp. 239-251.

[21] IEC Standard Publication 404-3: Methods of Measurements of Magnetic Properties by means of a single sheet tester.

[22] NAKATA, T.– KAWASE, J.: Accuracy of Measured Magnetic Field Stregth of Single Sheet Testers. [Publication IEC 68 WG 2.].

[23] NAFALSKI, A.–MOSES, A. J, Physica Scripta, 40, 1989, pp.532-535.

[24] GONDA, P. – TÓRÓK, J., Proccedings of the Conference SEITO, Gliwice 1993.

[25] ZEMÁNEK, I., Problematika automatizovaného měření parametrů magneticky měkkých materiálů. [Habilitační práce,] ČVUT FEL, 1994.

[26] ZEMÁNEK, I., Studies in Applied Electromagnetics and Mechanics 10 (1996), sp. issue Non-linear Electromagnetic Systems, IOS Press, OHM Ohmsha, Amsterdam, Oxford, Tokyo, Washington DC 1996, pp. 616-620.

[27] ZEMÁNEK, I. – HAVLÍČEK, V., Journal of Magnetism and Magnetic Materials, Vol. 304, Issue 2 (2006), Elsevier BV, Amsterdam 2006, pp. e577-e579.

[28] ZEMÁNEK, I. – NOVÁ, I., Proceedinds of the 3rd International Conference on Magnetism and Metalurgy WMM'08. Ghent (Belgium), 2008, pp. 413-429.

[29] ZEMÁNEK, I., Journal of Magnetism and Magnetic Materials, Vol. 254-255 (2003), Elsevier BV, Amsterdam 2003, pp.73-75.

[30] ZEMÁNEK, I., Journal of Electrical Engineering 55, No.10/S (2004), pp. 128-130.

[31] ZEMÁNEK, I., Proceedings of the VIth Latin American Workshop on Magnetism, Magnetic Materials and their Applications, Chihuahua (Mexico) 2003, p. 82.

[32] ZEMÁNEK, I., Journal of Electrical Engineering 57, No. 8/S (2006), pp.69-72.

[33] ZEMÁNEK, I., Proceedings of the International Symposium on Non-Linear Electromagnetic Systems, Cardiff (Wales, UK) 1995, p. D-48.

[34] ZEMÁNEK, I.: Proceedinds of the 10th International Workshop on 1&2 Dimensional Magnetic Measurement and Testing. Cardiff (UK), 2008, p. 26 (P-05).

[35] ZEMÁNEK, I., Proceedings of the Conference Magnetic Measurements 2004, Prague 2004, pp. 91-94.

[36] ZEMÁNEK, I., Proc. of the 3rd Japanese-Czech-Slovak Joint Seminar on Applied Electromagnetics, Brno - Praha, CSAEM, 1996, pp. 230-234.

[37] ZEMÁNEK, I. Przeglad Elektrotechnyczny (Electrical Review), R. 85 NR.1/2009, pp. 79-83.

[38] ŠÍPAL, V. – ZEMÁNEK, I. (supervisor), Proceedings of IEE Competition of Young Electrotechnicals, CTU, Prague 2006.

[39] YAMAMOTO, K. – HANBA, S., Journal of Magnetism and Magnetic Materials, Vol. 320 (2008), Issue 20, pp. e539-e541.

[40] HAVLÍČEK, V. – POKORNÝ, M., Journal of Magnetism and Magnetic Materials, Vol. 254-255 (2003), pp.76-78.

[41] ZEMÁNEK, I., Journal of Electrical Engineering 48, No.8/S (1997), pp. 120-122.

[42] ZEMÁNEK, I., Proc. of the Polish-Czech-Hungarian Workshop on Circuit Theory and Applications, Budapest (Hungary), 1997, pp. 106-109.

[43] ZEMÁNEK, I., Proceedings of the Conference Magnetic Measurements 2000, Prague 2000, pp. 15-20.

CURRICULUM VITAE

Doc. Ing. Ivan Zemánek, CSc.
Associate professor
Czech Technical University in Prague, Faculty of Electrical Engineering,
Department of Circuit Theory.
Technická 2, 166 27 Praha 6
zemanek@fel.cvut.cz

Born: September 11, 1952, Příbram

Education

1972 – 1977	Ing. (MSc.) – Czech Technical University in Prague, Faculty of Electrical Engineering, specialization: Communication technique (videofrequency technique)
1983	CSc. (PhD.) – Czech Technical University in Prague, Faculty of Electrical Engineering, branch: Radioelectronics
1995	Doc. (Associate professor) – Czech Technical University in Prague, Faculty of Electrical Engineering, branch: Theoretical Electrotechnique

Professinal career

1977 → …	Czech Technical University in Prague, Faculty of Electrical Engineering, Department of Circuit Theory
1977 – 1978	trainee (stage)
1978 – 1979	PhD student
1979 – 1995	assistant professor
1995 → …	associate professor

Sideline professinal activities

1986 – 1987	independent specialist – Astronomic Institute of the Czechoslovak Academy of Science (ČSAV).
1987 – 1989	independent researcher and advanced designer – Concern Grafotechna Prague – research, production.
1989 – 1991	independent scientist and researcher – Research Institute of Power Electrotechnics in Běchovice.

Pedagogical activities

- Continuous pedagogical practice at CTU (1979 – now): 30 years
  - Lectures: 22 years (1987 – now)
  - Exercises: 30 years (1979 – now)
- Lectured subjects: 12
- Exercised subjects: 21
- Guarantee of subjects: 9
- Author or co-author of subject plans: 5
- Member of the Commettee for Special Study (KME): 1
- Author /co-author of education programs for CAE: 8
- PhD students (ready): 4 (2)
- Student projects (diploma / bachelor works, other projects): 133
- Monographs: 2
- Textbooks: 7

Research activities

- Research of the bipolar logical integrated structures I^2L (integrated injection logic) – cooperation with Tesla Rožnov (1978 – 1984).
- Computer aided education (CAE) research at the CTU (1986 – 1990), 2x Rector CTU Price (1987, 1989).
- Soft magnetic materials measurements research (digital/analogue methods, digital control systems, measuring control algorithms) (since 1986). Design of special measuring systems for research and industry:
  - Rolling Works Frýdek-Místek
  - Research Institute of Ferrous Metallurgy Dobrá (in past)
  - Faculty of Electrical Engineering (FEE) CTU
  - Metalurgy Factory (Kovohutě) Rokycany

Research projects

- 1991 – 1993 colaborator of the CTU grant No. 8047
- 1993 – 1995 colaborator of the GACR grant No. 102/93/1197
- 1996 – 1998 colaborator of the GACR grant No. 102/96/1251
- 2001 – 2003 colaborator of the GACR grant No. 102/01/1335
- 2005 – 2011 co-manager of the research project
  No. MSM 6840770015 (supported by CTU grant and sponsored by the Ministry of Education, Youth and Sports of the Czech Republic).

Invited lectures (at conferences)

- 1994 University of Nagano (Japan)
- 1994 Doshisha University of Kyoto (Japan)

Membership in conference committees

- International conference committees: 11
- Czech conference committees: 1

Iternational stays

- Technische Universität Dresden (Germany)
- Universidad de Valencia (Spain)
- University of Nagano (Japan)

Publications

- Czech monographs: 2
- Papers in international reviewed journals (impacted): 11 (3)
- Papers at international conferences (in Proc.): 34
- Papers in Czech reviewed journals: 3
- Papers at Czech conferences (in Proc.): 10
- Patents / Usable Models: 1
- Realized projects (significant): 9 (2)
- Invited lectures at international conferences abroad: 2
- Cited works (ISI): 23 (2)
- Reviews for reviewed international journals (impacted): 9 (5)

Selected publications

- HAVLÍČEK, V. – POKORNÝ, M. – ZEMÁNEK, I.: Elektrické obvody 1. Monografie, Česká technika – nakladatelství ČVUT Praha, 2005. ISBN 80-01-03299-X. (14%)
- HAVLÍČEK, V. – ZEMÁNEK, I.: Elektrické obvody 2. Monografie, Česká technika – nakladatelství ČVUT Praha, 2008. ISBN 978-80-01-03971-7. (64 %)
- HAVLÍČEK, V.– ZEMÁNEK, I.: On-line AC Magnetic Measurements Accuracy. *Journal of Magnetism and Magnetic Materials*, Vol. 133 (1994), Elsevier BV, Amsterdam 1994, pp.399-401. ISSN 0304-8853. **IF 1,704** (50 %)
- ZEMÁNEK, I.: Exciting Signal Generator for SSTs. *Journal of Magnetism and Magnetic Materials*, Vol. 254-255 (2003), Elsevier BV, Amsterdam 2003, pp.73-75. ISSN 0304-8853. **IF 1,704** (100 %)
- ZEMÁNEK, I.– HAVLÍČEK, V.: Universal Control and Measuring System for Modern Classic and Amorphous Magnetic Materials Single/On-line Strip Testers. *Journal of Magnetism and Magnetic Materials*, Vol. 304, Issue 2 (2006), Elsevier BV, Amsterdam 2006, pp. e577-e579. ISSN 0304-8853. **IF 1,704** (60 %)

- ZEMÁNEK, I : Digital Control and Measuring System for Compensation Ferrometers. *Journal of Electrical Engineering* 45, No.8/S (1994), pp. 55-57. ISSN 0013-578X. (100 %)
- ZEMÁNEK, I.: Problems of the Computer Controlled Measuring Process of Soft Magnetic Materials at AC Magnetization. *Journal of Japan Society of Applied Electromagnetics*, special issue *Applied Electromagnetics in Materials* (1995), Tokyo 1995, pp. 239-251. ISSN 0919-4452. (100 %)
- ZEMÁNEK, I.: Non-linear Transformations for Soft Magnetic Material Measurements. *Studies in Applied Electromagnetics and Mechanics* 10 (1996), special issue *Non-linear Electromagnetic Systems*, IOS Press, OHM Ohmsha, Amsterdam, Oxford, Tokyo, Washington DC 1996, pp. 616-620. ISSN 1383-7281. (100 %)
- ZEMÁNEK, I.: Magnetic Flux Correction Based on the Adaptive Digital Feedback. *Journal of Electrical Engineering* 48, No.8/S (1997), pp. 120-122. ISSN 0013-578X. (100 %)
- ZEMÁNEK, I.: FFT Analyzer for New Compensated Single Strip Tester. *Journal of Electrical Engineering* 53, No.10/S (2002), pp. 73-76. ISSN 1335-3632. (100 %)
- ZEMÁNEK, I.: Magnetic Flux Correction Applied on New SST Measurements. *Journal of Electrical Engineering* 55, No.10/S (2004), pp. 128-130. ISSN 1335-3632. **(**100 %)
- ZEMÁNEK, I.: Software for Amorphous Materials Single Strip Testers. *Journal of Electrical Engineering* 57, No. 8/S (2006), pp.69-72. ISSN 1335-3632. (100 %)
- ZEMÁNEK, I.: Single sheet and On-line testing based on compensation method. *Przeglad Elektrotechnyczny (Electrical Review)*, R. 85 NR.1/2009, pp. 79-83, ISSN 0033-2097. **(**100 %)